

Jan Konrad Wallin

# Assessment of key microzooplankton species from Trondheimsfjorden using morphological and molecular methods

Graduate thesis in Marine Coastal Development

Supervisor: Nicole Aberle-Malzahn

August 2019



Tintinnid ciliate Picture: Jan Konrad Wallin



Jan Konrad Wallin

# Assessment of key microzooplankton species from Trondheimsfjorden using morphological and molecular methods

Graduate thesis in Marine Coastal Development  
Supervisor: Nicole Aberle-Malzahn  
August 2019

Norwegian University of Science and Technology  
Faculty of Natural Sciences  
Department of Biology







## Abstract

Microzooplankton (MZP) are heterotrophic and mixotrophic organisms in the size range of 20 - 200  $\mu\text{m}$ . The focus in this project was on the two main MZP groups, ciliates and heterotrophic dinoflagellates in Trondheimsfjorden. These groups are difficult to identify morphologically, making them a prime target for molecular identification methods. Molecular reference data for MZP species is scarce, especially from the Norwegian Sea incl. Trondheimsfjorden region. The MZP community was monitored intensively during a 13 weeks sampling series in spring 2019 with focus on species abundance, biomass and diversity. A peak in MZP abundance and biomass was observed in April with total of 27160 cells  $\text{L}^{-1}$  and 126  $\mu\text{g C L}^{-1}$ , respectively Ciliates dominated the beginning of the sampling series while dinoflagellates increased in abundance and biomass towards the end. The ciliate *Laboea strobila* was characterised as a key species in terms of biomass within the spring MZP community in Trondheimsfjorden. The most diverse genus found was *Protoperidinium* with 12 morphospecies identified. In addition to the intensive spring sampling in 2019, MZP cells from Trondheimsfjorden were isolated during spring, summer and autumn 2018 to obtain molecular data for identification. A working protocol for single-cell isolation and DNA amplification of MZP species from Trondheimsfjorden was developed. The final protocol showed a PCR success rate of 26,5 percent. 23 MZP sequences were obtained and used for molecular identification. In total, six sequences were retrieved for *L. strobila* from both 18 and 28s molecular markers. Although key MZP species were identified by both morphological and molecular methods, work remains in order to optimise the application and use of molecular methods for MZP identification.

## Sammendrag

Mikrozooplankton (MZP) er heterotrofiske og mixotrofe organismer i størrelsesområdet 20 - 200  $\mu\text{m}$ . Disse organismene er vanskelige å artsbestemme med molekylære identifikasjonsmetoder. Det er mangelfullt med referansedata fra Trondheimsfjorden. Fokus i dette prosjektet var de to viktigste MZP-gruppene, ciliater og dinoflagellater i Trondheimsfjorden. MZP-samfunnet ble overvåket i løpet av en 13 ukers prøvetakingsserie i vår 2019 med fokus på overflod, biomasse og artsmangfold. En topp i MZP-forekomst og biomasse ble observert på juledag 120 med totalt  $27160 \text{ celler L}^{-1}$  og  $126 \text{ ug C L}^{-1}$ . Ciliater dominerer begynnelsen av prøvetakingsserien, mens dinoflagellater øker i antall og biomasse mot slutten. *Laboea strobila* var den dominante arten når det gjaldt biomasse, og ble karakterisert som en nøkkelart i vårsesongens MZP-samfunn. Den mest artsrike slekten var *Protoperidinium* med 12 morfologiske arter identifisert. MZP-celler fra Trondheimsfjorden ble isolert i vår-, sommer-, og høstsesongen 2018 for å innhente molekylære data for artsidentifisering. En protokoll for isolasjon av enkeltceller og DNA-amplifisering av MZP-arter fra Trondheimsfjorden ble utviklet. Den endelige protokollen viste en PCR suksessrate på 26,5 prosent. 23 sekvenser ble innhentet og deretter brukt til molekylær identifikasjon av MZP arter. Totalt ble seks sekvenser innhentet for *L. strobila* fra både 18s og 28s molekylære markører. Selv om viktige MZP-arter ble identifisert ved både morfologiske og molekylære metoder, gjenstår det arbeid for å optimalisere anvendelsen av molekylære metoder for identifikasjon av MZP.

## **Acknowledgements**

My main supervisor for this project has been Nicole Aberle-Malzahn, I would like to thank her for the excellent guidance and encouragement I have received during my project. I would also like to thank the co-supervisors for my project, Sanna Majaneva, who has greatly helped me through the molecular challenges I have been facing, and Katharina Bading, for much appreciated help with sampling, single-cell isolation, and MZP quantification.

I would also like to thank the people at Trondhjem Biological Station and Mari-Ann Østensen especially for all the guidance and help in the genetics lab.

In addition, I would like to thank Torbjørn Ekrem for advice in relation to DNA barcoding and Markus Majaneva for sharing his expertise on molecular methods for protist.

Luka Supraha from UiO also deserves acknowledgement for kindly sharing his methods.

I would like to thank my colleagues from the biology programme, Håvard, Øystein and Martin, for valuable input on my work.

Finally, I want to thank Stefanie for all the love and support she has given me during this longer-than-expected project.



# Table of contents

<b>ABSTRACT</b> .....	<b>III</b>
<b>PREFACE</b> .....	FEIL! BOKMERKE ER IKKE DEFINERT.
TABLE OF CONTENTS .....	VII
APPENDIX A: MICROZOOPLANKTON SPECIES ISOLATED DURING AUTUMN 2018.....	VIII
LIST OF FIGURES .....	VIII
LIST OF TABLES.....	IX
ABBREVIATIONS .....	X
<b>1. INTRODUCTION</b> .....	<b>11</b>
1.1. MICROZOOPLANKTON.....	11
1.2. PLANKTONIC FOOD WEBS.....	11
1.3. MICROZOOPLANKTON METHODS.....	12
1.4. MICROZOOPLANKTON IN TRONDHEIMSFJORDEN .....	14
1.5. AIMS .....	14
<b>2. METHODS</b> .....	<b>14</b>
2.1. SAMPLING .....	16
2.2. QUANTITATIVE ASSESSMENT OF MZP COMMUNITY .....	17
2.2.1. <i>Microzooplankton quantification</i> .....	17
2.2.2. <i>Morphological identification</i> .....	17
2.2.3. <i>Biovolume calculation</i> .....	17
2.3. MOLECULAR METHODS .....	18
2.3.1. <i>Protocol development</i> .....	18
2.3.2. <i>Single-cell isolation</i> .....	21
2.3.3. <i>PCR</i> .....	22
2.3.4. <i>DNA analysis</i> .....	22
2.3.5. <i>Sequence analysis</i> .....	22
<b>3. RESULTS</b> .....	<b>24</b>
3.1.1. <i>Quantitative assessment of MZP community Abundance and biomass</i> .....	24
3.1.2. <i>Diversity</i> .....	33
3.2. MOLECULAR ANALYSIS .....	35
3.2.1. <i>Protocol development</i> .....	35
3.2.2. <i>Single cell isolation</i> .....	35
3.2.3. <i>BLAST identification</i> .....	36
3.2.4. <i>Phylogenetics</i> .....	39

<b>4.</b>	<b>DISCUSSION .....</b>	<b>43</b>
4.1.	MICROZOOPLANKTON COMMUNITY ASSESSMENT DURING SPRING 2019.....	43
4.2.	MOLECULAR SPECIES IDENTIFICATION OF MICROZOOPLANKTON .....	46
4.3.	METHODOLOGY.....	48
<b>5.</b>	<b>CONCLUSION AND OUTLOOK .....</b>	<b>50</b>
<b>6.</b>	<b>LITERATURE.....</b>	<b>52</b>

## **Appendix A: Microzooplankton species isolated during autumn 2018**

### **List of figures**

Figure 1: Map of Trondheimsfjorden with the position of TBS made with QGIS Desktop 3.4.11 software using the Natural Earth quick start kit package. ....	15
Figure 2: Washing of a Lugol fixed <i>Laboea strobila</i> cell with a thiosulphate solution (1950 $\mu\text{g Na}_2\text{S}_2\text{O}_3 \text{ mL}^{-1}$ ). Pictures show the same cell before (a) and right after (b) addition of thiosulphate. ....	19
Figure 3: Schematic showing steps in the single-cell isolation protocol. The figure was made with ScienceDraw 8.7.5 software.....	21
Figure 4: Dinoflagellate (a) and ciliate (b) abundance ( $\text{Cell L}^{-1}$ ) and biomass ( $\mu\text{g C L}^{-1}$ ) during a 84 day sampling series in spring 2019 with 13 sampling dates (Julian days; Month). ....	24
Figure 5: Relative abundance (a) and biomass (b) of ciliates (light gray) and dinoflagellates (dark gray) during a 84 day sampling series in spring 2019 with 13 samples (Julian days; Month).....	26
Figure 6: Relative abundance of three size classes, $<25\mu\text{m}$ , $25\text{-}50 \mu\text{m}$ and $>50 \mu\text{m}$ , of dinoflagellates (a) and ciliates (b) during a 84 day sampling series (Julian days; Month) in spring 2019.....	27
Figure 7: Relative biomass of three size classes, $<25\mu\text{m}$ , $25\text{-}50 \mu\text{m}$ and $>50 \mu\text{m}$ of dinoflagellates (a) and ciliates (b) during a 84 day sampling series (Julian days; Month) in spring 2019.....	29

Figure 8: Abundance (Cells L<sup>-1</sup>) and Shannon Weaver diversity index (H') (A) as well as biomass (µg C L<sup>-1</sup>) (B) of dinoflagellates and ciliates during a 84 day sampling series (Julian days; Month) in spring 2019 ..... **Feil! Bokmerke er ikke definert.**

Figure 9: A selection of species from spring 2019 sampling series and 2018-2019 single cell isolation. Molecular data was obtained for the species marked with a black border. Undetermined tintinnid ciliate (A), *Tintinnopsis* sp. (B), Undetermined tintinnid ciliate (C), *Scrippsiella* cf. *trochoidea* (D), *Gymnodinium* cf. *helveticum* (E), *Laboea* cf. *strobila* (F), *Protoperidinium* cf. *depressum* (G), *Gyrodinium* cf. *spirale* (H), *Strombidium* cf. *wulffi* (I), *Mesodinium* cf. *rubrum* (J), *Strombidium* sp. “20 – 32 µm” (K). Live (A-C, G) and Lugol-fixed (D-F,H-K) specimens. Photos taken with Leica DM IRB Inverted microscope (20x objective)..... 32

Figure 10: 28 s phylogram (Maximum Likelihood, 500 bootstraps, support threshold) comprising of ciliate single cells isolation sample sequences (denoted as sample followed by a two or three digit number) in addition to sequences downloaded from Genbank. Branch values are bootstrap percentages. .... 39

Figure 11: 18 s phylogram (Maximum Likelihood, 500 bootstraps, support threshold) comprising of ciliate SCI sample sequences (denoted as “sample” followed by a two digit number) in addition to sequences downloaded from Genbank. Branch values are bootstrap percentages. .... 41

Figure 12: 18 s phylogram (Maximum Likelihood, 500 bootstraps, support threshold) comprising of dinoflagellate SCI sample sequences (denoted as sample followed by a two digit number) in addition to sequences downloaded from Genbank. Three tintinnid samples are used as an outgroup (samples 67, 69 and 71). Branch values are bootstrap percentages. . 42

Figure 13: Live specimens of dominant species from the autumn 2018 season. Specimens were isolated with single-cell isolation. *Protoperidinium* sp. (A), *Protoperidinium* sp. (B), *Tiarina* cf. *fuscus* (C), *Euplotes* sp. (D), *Gyrodinium* cf. *spirale* (E), *Salpingella* sp. (F) and undetermined tintinnid ciliate (G). Photos taken with Leica DM IRB inverted microscope (20x objective)..... 57

## List of tables

Table 1: Primers tested during protocol development with the number of samples run in PCR in addition to number of samples that yielded bands in Gel-electrophoresis..... 20

Table 2: PCR master mix reagents tested in protocol development the number of samples run in PCR in addition to number of samples that yielded bands in Gel-electrophoresis..... 20

Table 3: PCR programs tested during protocol development. .... 21

Table 4: List of ciliates and dinoflagellates identified from the sampling series including size category, maximum abundance, peak timing, mean biovolume, and mean carbon content of each taxon..... 33

Table 5: BLAST query results with morphological identity, picture reference, BLAST identify with accession number, query cover and identity. .... 37

## Abbreviations

<b>MZP</b>	Microzooplankton
<b>DOM</b>	Dissolved organic matter
<b>DNA</b>	Deoxyribonucleic acid
<b>TBS</b>	Trondhjem biological station
<b>PhD</b>	Doctor of Philosophy
<b>PBS</b>	phosphate-buffered saline
<b>TE</b>	Tris-Ethylenediaminetetraacetic acid
<b>PCR</b>	Polymerase chain reaction
<b>MM</b>	Master mix
<b>JD</b>	Julian days
<b>μL</b>	Microliter
<b>μm</b>	Micrometer
<b>BLAST</b>	Basic Local Alignment Search Tool
<b>SCI</b>	Single-cell isolation
<b>MCL</b>	Maximum composite likelihood
<b>kb</b>	Kilobase

# 1. Introduction

## 1.1. Microzooplankton

Microzooplankton (MZP) is most commonly referred to as a group of mixotrophic and heterotrophic plankton in the size range of 20 - 200  $\mu\text{m}$  (Sieburth et al. 1978). This definition has often been adapted to include all protists and metazoans below 200  $\mu\text{m}$  (Calbet, 2008; Calbet & Alcaraz, 2009). Thus, MZP consists of protozoans such as ciliates, dinoflagellates, flagellates, foraminiferans, and radiolarians and metazoans including rotifers, copepod nauplii and meroplanktonic larvae (Calbet & Alcaraz, 2009). Ciliates and heterotrophic dinoflagellates were the focus of this thesis and here these two groups together will be referred to as microzooplankton (MZP).

Ciliates along with heterotrophic dinoflagellates are considered as the main groups of MZP due to their trophic role as primary grazers of phytoplankton and their overall abundance in the plankton, some groups being able to form blooms (Calbet & Alcaraz, 2009; Johnson & Stoecker, 2005). MZP grazing has been proved to be the cause for more than half of the phytoplankton mortality per day in oceans (Calbet & Landry, 2004). MZP, ciliates especially, have faster growth rates and responses to shifts in abiotic conditions than metazoans (Calbet & Landry, 2004). These rapid growth rates translate into high grazing rates on phytoplankton prey during spring bloom events (Montagnes, 1996). The massive grazing and fast growth responses of MZP affirm their part as a major part of the food web as the link between primary producers and higher trophic levels.

## 1.2. Planktonic food webs

Phytoplankton productivity varies across the world's oceans and is linked to the availability of nutrients in the euphotic zones (Aberle et al. 2007). It is especially in coastal areas where seasonal mixing brings nutrient-rich water up from the depths towards the photic zone. The nutrient-rich water in addition to increased light in spring provides good conditions for photosynthesis. A massive increase in photosynthesis in phytoplankton in the springtime leads to a phenomenon referred to as the spring bloom (Tokle, 1999). The spring bloom is an important event for communities in temporal coastal areas and the effects of the spring bloom production is reflected in higher trophic levels as through grazing on the blooming phytoplankton.

The term microbial loop describes an alternative trophic pathway of carbon at the base of marine food webs which stands on contrast to classical trophic pathways leading up the food chain (Sieburth et al. 1978). Primary production and secondary production of planktonic communities produce waste in the form of particulate organic matter (POM) in the form of dead cells and tissue in addition to faecal matter. A large part of POM is lost from the water column through sedimentation (Sieburth et al. 1978). Planktonic bacteria attach themselves to POM breaking it down before it sediments out of the water column. This creates the basis for the microbial loop (Pomeroy et al. 2007). In addition to POM a large part of the microbial loop is driven by dissolved organic matter (DOM). Up to 50 percent of carbon fixed by primary producers is released as DOM (Azam et al. 1983). DOM is also utilised by bacterial plankton which are preyed upon by heterotrophic nanoflagellates which in turn are prey for MZP. DOM released through the steps of the microbial loop acts as a feedback, justifying the characterisation as a loop. Carbon from the microbial loop will also be taken up in other parts of the planktonic food web through predation from mesozooplankton. Thus, carbon from the microbial loop feeds into the classical trophic food web forming a link between these two systems (Pomeroy et al. 2007). The microbial loop enables recycling of carbon above the thermocline in contrast to grazing on phytoplankton by mesozooplankton where a larger part of the carbon will be lost from the euphotic zone through sinking faecal matter (Sieburth et al. 1978).

Both being key parts of the planktonic food web, heterotrophic dinoflagellates and ciliates do have differences when it comes to grazing strategies. Ciliates graze primarily on single-celled organisms that are small relative to their body size while dinoflagellates are known to prey upon larger organisms such as chain-forming diatoms (Calbet, 2008). Many dinoflagellates and some ciliate species are considered mixotrophic, sequestering plastids from preyed phytoplankton to obtain energy and carbon photosynthetically (Johnson & Stoecker, 2005). Although most mixotrophic species are to a large extent dependent on heterotrophic growth strategies some species like *Mesodinium spp.* are able to utilise dissolved nutrient and maintain photosynthetic rates that are high enough to form blooms (Johnson & Stoecker, 2005).

### **1.3. Microzooplankton methods**

Traditional methods to study MZP have mostly been done through microscopy with either live or fixed specimens. Preservation methods such as Lugol's iodine solution (Lugol) are

commonly used for quantitative studies while cytological staining methods are required to uncover key morphological features for a proper taxonomic identification e.g. of ciliates (Agatha, 2011). While morphological methods of identification often are less time consuming than molecular methods, there are risks of misidentification due to poor reference literature, experience bias and low sample quality.

While molecular methods are well established for metazooplankton, there is lack of molecular methods for MZP due to the difficulties related to the small size of the target organisms. While DNA can be extracted and purified from most plankton, these methods require more than one specimen in order to yield enough template DNA (Marín et al. 2001). Using several cells for isolation in order to obtain enough template DNA is feasible when numerous similar cells are readily available. This method, however, cannot be used for rare species and species which are not easily cultivated. Another method to obtain DNA from MZP is single-cell isolation (SCI), where one or a few cells are isolated directly for DNA amplification with few DNA extraction steps (Marín et al. 2001; Ki et al. 2005). The most used DNA regions for the study of MZP has been within the nuclear rDNA. The small 18S subunit (SSU) and large 28S subunit (LSU) of rDNA have been widely used for both species identification and phylogenetic analysis at a higher level due to the high conservation in regions within these markers (Edwardsen et al. 2003).

In food web ecology, analysis of gut content is considered as an established method to map trophic interactions in larger animals (Roslin & Majaneva, 2016). Morphological gut content analysis can often lead to observation bias due to different prey organisms having varying robustness and therefore digestion rates (Montagnes et al. 2010). Molecular methods such as quantitative polymerase chain reaction (qPCR) have successfully been used to detect MZP in gut contents although it was suggested that the development of MZP specific primers was needed in order to improve overall MZP detection (Töbe et al. 2009).

Molecular methods with the use of specific genetic markers for the identification of plants and animals has in the later years proven to be an important tool in addition to morphological methods for species identification (Hebert et al. 2003; Pawlowski et al. 2012). In recent years protozoans have been given more attention, especially in the light of the advances taking place in the fields of molecular ecology and DNA barcoding enabling new methods to be applied to these otherwise difficult taxa (Pawlowski et al. 2012). Given the complex methods

of morphological identification of certain MZP taxa, molecular methods are considered to advance taxonomic identification of MZP, thus enabling more accurate and less time-consuming identification of species.

#### **1.4. Microzooplankton in Trondheimsfjorden**

The MZP community in Trondheimsfjorden has in the past been subject to research in the past. Tokle (1999) describes nutrient transfer in the zooplankton community of Trondheimsfjorden. With focus on ciliates as the protozoan component of the zooplankton community, species composition and abundance is described. Aloricate ciliate species such as *Mesodinium rubrum* and *Laboea strobila* are highlighted as abundant in the spring season (Tokle, 1999).

#### **1.5. Aims**

The overarching aim for this project is to characterise the MZP community in Trondheimsfjorden and to look into how molecular methods can be used in addition to morphological methods. More detailed aims with intermediate objectives are:

1. Characterisation of the MZP community in Trondheimsfjorden through traditional methods of identification and quantification of MZP:
  - Monitoring of the MZP community during a spring bloom period.
  - Determining key MZP species occurring in Trondheimsfjorden.
2. Molecular identification of MZP species from Trondheimsfjorden:
  - Development of a working protocol for molecular identification of MZP species
  - Isolation of key species and obtaining barcode sequences for molecular identification of these species.
3. Comparison of the molecular identification method to traditional methods for use in Trondheimsfjorden

## **2. Methods**

The study area for this thesis was Trondheimsfjorden with one sampling station located at Trondhjem Biological Station (TBS, figure 1, (63°26'27.0"N, 10°20'56.5"E) Trondheimsfjorden is one of the longest fjords in Mid-Norway with a total length of 126 kilometres. The fjord has four main sills that divide three main basins; Ytterfjorden,

Midtfjorden and Beitstadfjorden. The three innermost sills are sufficiently deep to not reduce the water circulation in the fjord while the shallow areas at the mouth determine water mass exchange between Trondheimsfjorden and the Norwegian Sea (Bakken, 2000). Trondheimsfjorden is a typical Norwegian fjord with sills affecting the water transport in and out of the fjord and with substantial freshwater run-off.

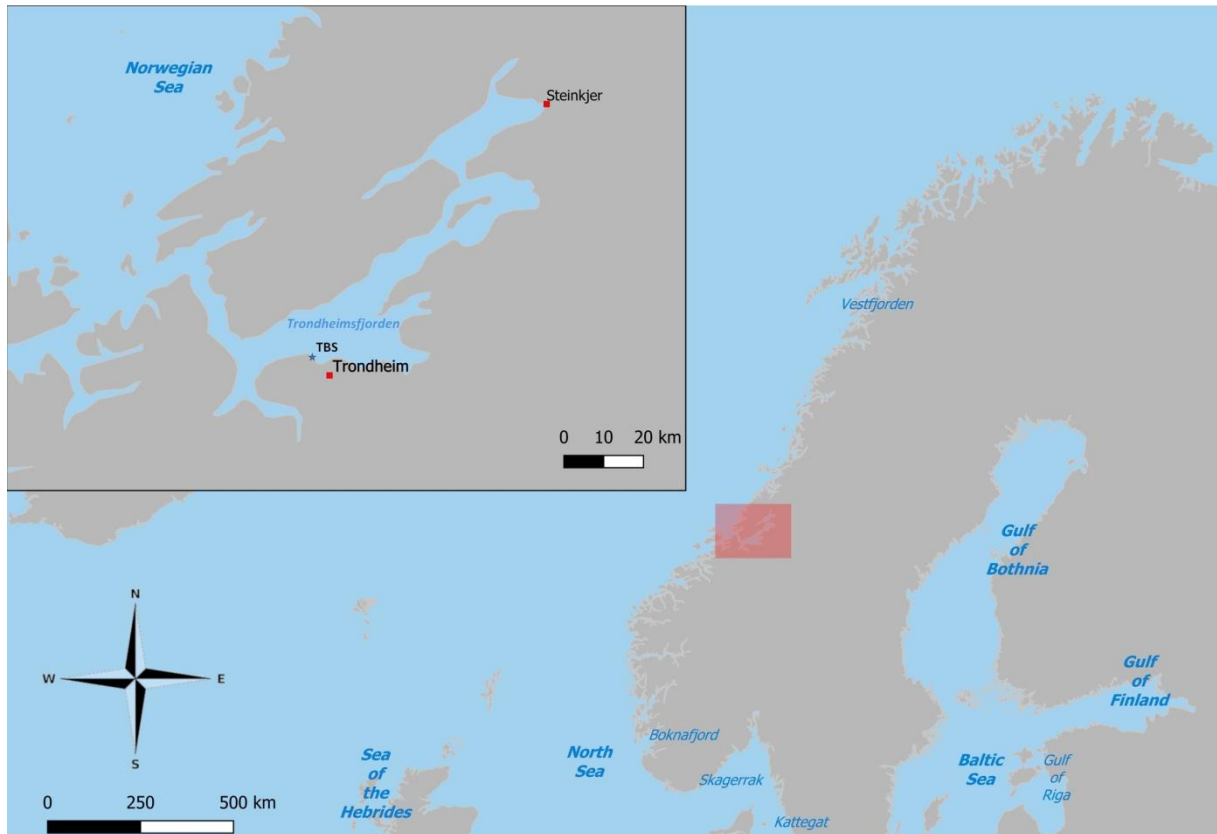


**Figure 1:** Map of Trondheimsfjorden with the position of TBS made with QGIS Desktop 3.4.11 software using the Natural Earth quick start kit package.

Seawater influx in Trondheimsfjorden is mainly from two different sources, one being Atlantic water and the other being the Norwegian coastal current (Bakken et al. 2000). In the winter, Atlantic water flows into the fjord and down into the basins pushing the basin water masses up during the summer season. The second dominant influx of seawater begins in the autumn where water masses from the Norwegian coastal current get pushed towards the shore and into the fjord. This seawater influx leads to an exchange of mid water above the sill and out of the fjord. Convection between the different water masses in the fjord is constantly taking place to a certain degree with the autumn influx of coastal water especially affecting deeper layers. In addition to saline water mass exchanges in the fjord there is also a substantial runoff from freshwater drainages around the fjord. During the melting season in spring, freshwater runoff creates a brackish layer of water at the surface. In addition to the

water exchange, freshwater influx, and the seasonal dynamics, additional forces like current systems and wind affect the mixing and characteristics of Trondheimsfjorden water masses (Bakken et al. 2000).

Seasonal patterns in salinity and temperature can be observed in Trondheimsfjorden. Like most fjords, Trondheimsfjorden is affected by the physical isolation from the ocean, which greatly impacts the salinity and temperature throughout the year. Salinity below 30 can be observed in the brackish surface layer that is present in the outer parts of the fjord during the summer season. Atlantic seawater which enters the fjord in early winter usually has a salinity of 34,7-34,8. The deepwater temperature remains below 7,5 °C throughout the year while disruption of the stratification in winter causes lower temperatures at surface level (Bakken et al. 2000).

The pier at TBS was chosen as the main sampling station for this project. The station was chosen as it was already part of a well-established and on-going sampling series conducted by Katharina Bading as a part of her PhD project. The sampling series was carried out over 2 to 3 years with weekly sampling efforts in order to monitor and analyse seasonal phenology in MZP. Additional advantages of the sampling station are ease of sampling throughout the year, proximity to laboratory facilities and increased possibility for instantaneous sampling. The current system at TBS comprises of currents coming from the outer part of the fjord mixed with water dominated by freshwater runoff from the Orkla and Gaula river systems. In addition, there is a proximity of a tidal vortex created from the outflow of the river Nidelven (Bakken et al. 2000). The sampling station TBS is thought to be representative of typical conditions for Trondheimsfjorden being affected by both the outside ocean and the large freshwater influences.

## **2.1. Sampling**

Samples were collected from January 2018 to end of May 2019. In spring 2019, an intensive MZP spring sampling campaign was conducted, where 13 weekly samples from 19<sup>th</sup> of February to 14<sup>th</sup> of May 2019 were analysed. Seawater was collected once per week with a water column sampler from a depth of 3-4 meters at high tide. The collected seawater was fixed in two individual samples, one with acidic and one with neutral Lugol's iodine solutions (Karlson et al. 2010). The samples were stored in brown 200mL glass bottles for later analysis. Additional seawater collected during the weekly sampling was used for isolation of

MZP cells for molecular analysis. The seawater was brought to the plankton laboratory at TBS for further examination and molecular analysis. During peak bloom periods, additional samples were collected by net tows with a plankton net (20 cm diameter, 20 µm mesh size) were taken throughout the whole water column to sample additional MZP cells for molecular analysis.

## **2.2. Quantitative assessment of MZP community**

### **2.2.1. Microzooplankton quantification**

Fixed samples were analysed using Utermöhl's plankton sedimentation and microscopy methods (Utermöhl, 1958). Samples were settled in settling chambers for a minimum of 24 hours before analysis with a Leica DM IRB inverted microscope. The settling volume used was 100mL and changed to 50mL settling chambers when total MZP cell counts exceeded 400 cells of the most abundant species in the counting chamber. In order to establish a photo library for the taxa identified and a basis for cell biovolume calculations, all MZP cells from 8 out of 13 settled samples were photographed. Photographs were taken using Zeiss Zen 2.3 Imaging software for microscopy. Pictures taken were used as a standard identification reference for counting of the remaining samples

### **2.2.2. Morphological identification**

Taxa were identified using available literature. Loricated ciliates were identified according to data sheets from the Planktonic Ciliate project ([www.zooplankton.cn](http://www.zooplankton.cn)). Aloricate ciliates and dinoflagellates were identified using the marine microzooplankton manual of the North Sea (Löder & Haunost, 2009) in addition to Yang et al. (2014), Kraberg et al. (2010), Larink & Westheide (2006), and the Planktonic Ciliate project ([www.zooplankton.cn](http://www.zooplankton.cn)).

### **2.2.3. Biovolume calculation**

Between 1 and 57 cells from each taxa were measured according to the three-dimensional shape of each taxa using ImageJ 1.8.0 software (Rueden et al. 2017). Dinoflagellates shapes were determined according to Hillebrandt et al. (1999) and Sun & Liu (2003). For ciliates, overall shapes were derived from Sun & Liu (2003) and assigned to each taxa according to similarity. Average biovolumes for each taxa were derived from the calculations of individual cell measurements and carbon contents per cell were calculated from these averages (Sun & Liu, 2004).

## 2.3. Molecular methods

### 2.3.1. Protocol development

A single-cell isolation protocol based on Edvardsen et al. (2003) was developed further to increase the success rate as initial tests yielded no results. MZP cells from natural samples, Lugol-fixed samples and ciliate cultures. The *Euplotes sp.* ciliate cultures were kept at 15 °C and fed with *Rhodomonas*. Three different washing solution were used during the protocol development. As a part of the protocol development several different solutions were tested for the washing and cell fixation steps. Phosphate-buffered saline (PBS) and Tris-Ethylenediaminetetraacetic acid (TE) buffer solutions were tested for the washing step in addition to filtered and autoclaved saltwater and autoclaved freshwater and MQ-water (Ki et al. 2004). For pre-PCR cell fixation, MQ-water, ethanol (95 %), TE-buffer and PCR master mix were tested. The different washing and fixation solutions were cross-tested. To limit stress due to heat during the single-cell isolation, glass slides and solution stocks were kept on ice.

Isolation from Lugol-fixed samples was attempted in order to obtain additional microzooplankton samples. To neutralise the iodine which may act as an inhibitor in the DNA amplification method (Auinger et al. 2008), Lugol samples were sedimented and subsequently washed with filtered and autoclaved seawater twice in settling chambers. Cells were then picked from the settling chamber well and isolated in the same manner as with live MZP cells. Another method was to isolate MZP cells from Lugol-fixed samples and using a thiosulphate (1950 µg Na<sub>2</sub>S<sub>2</sub>O<sub>3</sub> mL<sup>-1</sup>) solution as a washing solution (figure 2).

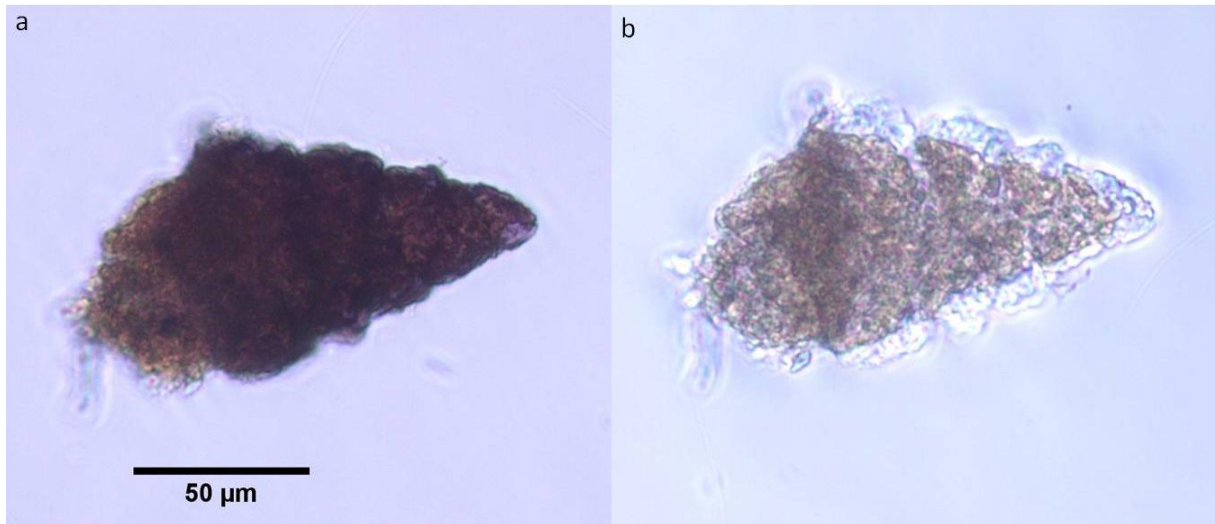


**Figure 2:** Washing of a Lugol fixed *Laboea strobila* cell with a thiosulphate solution ( $1950 \mu\text{g Na}_2\text{S}_2\text{O}_3 \text{ mL}^{-1}$ ). Pictures show the same cell before (a) and right after (b) addition of thiosulphate.

An alignment with different primers along with available MZP sequences was created to determine which primers would work well for MZP. A combination of the F1 and 18scom R1 primers (table 1) was determined to be a good fit with both dinoflagellates and ciliates and was chosen for testing.

PCR protocol based on Edvardsen (2003) was further developed. The reaction was optimised by cross testing volumes, reagents and different cycle programs (table 2; table 3). Both 25 and 50  $\mu\text{L}$  total PCR volumes were used in addition to different concentrations of primers and nucleotides. Condition altering reagents such as Dimethyl sulfoxide (DMSO), Magnesium ( $\text{Mg}^+$ ), Proteinase K and Kilo Base Extender were also cross -tested to help optimising PCR. An annealing gradient PCR was run to find optimal temperature.

A portion of the samples were isolated with a double set of primers for 18 and 28s in order to run a nested PCR and retrieve sequences from two genes out of each sample (Edvardsen et al. 2003). The positive PCR products from the nested PCR were amplified with 18 and 28s primers separately to obtain products from both genes.

**Table 1:** Primers tested during protocol development with the number of samples run in PCR in addition to number of samples that yielded bands in Gel-electrophoresis.

Primer pair	Region	Forward	Reverse	Samples	Gel
<b>18ScomF1/R1<sup>a</sup></b>	18s	GCTTGTCTCAAAGATTAAGCC ATGC	CACCTACGGAAACCTTGT TACGAC	104	7
<b>Dino18s F1/R1<sup>a</sup></b>	18s	AAGGGTTGTGTTYATTAGNTA CAC	GAGCCAGATRCDCACCC A	3	-
<b>F1/1528r<sup>b</sup></b>	18s	GCTTGTCTCAAAGATTAAGCC ATGC	CACCTACGGAAACCTTGT TC	130	39
<b>F1/18scom R1<sup>a,b</sup></b>	18s	CACCTACGGAAACCTTGTTAC GAC	CACCTACGGAAACCTTGT TACGAC	42	-
<b>DIR-F/D2C-R<sup>b</sup></b>	28s	ACCCGCTGAATTTAAGCATA	CCTTGGTCCGTGTTTCAA GA	29	13

<sup>a</sup>From Lin et al. (2006).

<sup>b</sup>From Edvardsen et al. (2003).

**Table 2:** PCR master mix reagents tested in protocol development the number of samples run in PCR in addition to number of samples that yielded bands in Gel-electrophoresis.

Master mix	Volume(μL)	Polymerase	Mg <sup>+</sup> (μL)	Kb extender (μL)	Proteinase K (μL)	DMSO (μL)	Samples	Gel results
<b>1</b>	25	Dynazyme II	-	-	-	-	4	-
<b>2</b>	25	Phire Hot start ii	-	-	-	-	50	7
<b>3</b>	25	Phire Hot start ii	-	-	-	0,6-1,2	28	-
<b>4</b>	50	Phire Hot start ii	-	-	-	1,2	2	-
<b>5</b>	25	Phire Hot start ii	-	-	1,3	1,2	7	-
<b>6</b>	50	Phire Hot start ii	1	-	-	2,5	7	-
<b>7</b>	50	Phire Hot start ii	1	-	2	2-2,5	12	-
<b>8</b>	50	Platinum Taq	2	4,5	-	-	124	39

**Table 3:** PCR programs tested during protocol development.

Program	Annealing temperature (°C)	Cycles	Samples tested	Positive Results
1	50-55	35	9	-
2	50	35	56	7
3	58 - 68	35	12	12
4	65	35	17	-
5	65	50	13	-
6	55	40	124	39

### 2.3.2. Single-cell isolation

Single live MZP cells randomly picked from seawater samples were isolated in order to run single cell PCR. Single-cell isolation protocol was modified after Edvardsen et al. (2003). Cells were picked from seawater samples looking through a Leica M205 C stereo microscope and placed in a smaller drop of sample water (Figure 3). Single cells were picked from the sample using a capillary mouth pipette and deposited on a glass slide in a drop of sample water. The glass slide was then transferred to a reverse microscope and photographed. The cell was then transferred to a new drop of Milli-Q water in order to wash the cell. The washing step was repeated three times before transferring the cell into a drop of PCR master mix (MM). The MM drop containing the cells was then transferred to a 200 $\mu$ L PCR tube. After isolation, PCR-tubes containing samples were incubated at 80 °C for 2 minutes before storing at -20 °C.

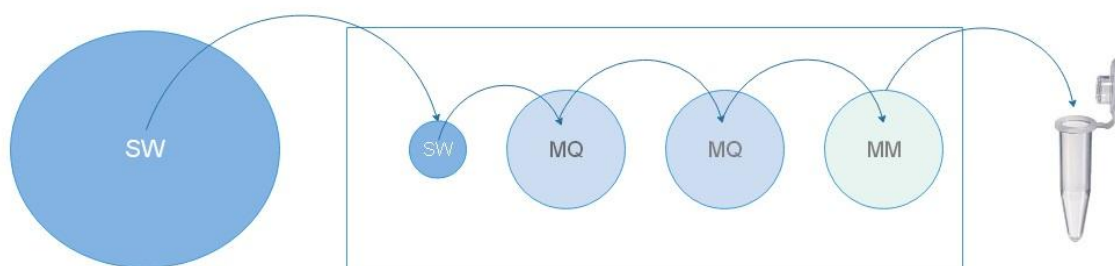


**Figure 3:** Schematic showing steps in the single-cell isolation protocol. The figure was made with ScienceDraw 8.7.5 software.

Single cell isolation from Lugol-fixed samples was performed in the same manner as for live material but with a Thiosulphate solution ( $1950 \mu\text{g Na}_2\text{S}_2\text{O}_3 \text{ ml}^{-1}$ ) as a replacement for Milli-Q water in the washing step (Auinger et al. 2008).

### 2.3.3. PCR

DNA from isolated MZP cells was amplified using MZP specific primers. 18 and 28s molecular markers were chosen based on the reference data and protocols available. Primer pair 1F (5' - AAC CTG GTT GAT CCT GCC AGT) and 1528R (3' - TGA TCC TTC TGC AGG TTC ACC TAC) was used to amplify the 18s rRNA gene while the DIR-F (5' - ACC CGC TGA ATT TAA GCA TA) and D2C (3' - CCT TGG TCC GTG TTT CAA GA) primer pair was used to amplify the D1 and D2 region of the 28s rRNA gene (Edwardsen et al. 2003). For each isolated sample, 0,4 uL of Invitrogen™ Platinum™ Taq DNA Polymerase in addition to Milli-Q water was added for a 50  $\mu\text{L}$  total PCR volume. PCR reactions were performed using a SimpliAmp Thermal Cycler using a program specific for the polymerase (table 3; program 6).

### 2.3.4. DNA analysis

PCR products were run on a 1,5 percent agarose gel in 1xTAE buffer with a SYBR™ Safe DNA Gel Stain. Positive PCR products were cleaned using an illustra GFX PCR DNA and Gel Band Purification Kit and purified products were then sent for forward and reverse Sanger sequencing.

### 2.3.5. Sequence analysis

Sequence chromatograms were visually checked and trimmed in Chromas 2.6.6 software (Technelysium Pty Ltd, 2018). Sequence assembly and alignment editing was done in BioEdit 7.0.5.3 software (Hall, 1999) and alignment was done using the MAFFT version 7 online service (Kato et al. 2017). Sequences were assembled in three separate alignments: Dinoflagellate 18s; Ciliate 18s, and Ciliate 28s. Final base pair lengths for the three alignments were approximately 1.6 kb, 1.5 kb, and 0.6 kb respectively. Phylogenetic analysis was done using Mega-X 10.0.5 software (Kumar et al. 2018).

The evolutionary history was inferred by using the Maximum Likelihood method and General Time Reversible model (Nei & Kumar, 2000). The bootstrap consensus tree inferred from 500 replicates (Felsenstein, 1985). Branches corresponding to partitions reproduced in less

than 50% bootstrap replicates were collapsed. Initial tree for the heuristic search were obtained automatically by applying Neighbor-Join and BioNJ algorithms to a matrix of pairwise distances estimated using the Maximum Composite Likelihood (MCL) approach, and then selecting the topology with the highest log likelihood value. For the dinoflagellates, the 18s analysis involved 81 nucleotide sequences and there were a total of 1624 positions in the final dataset. For ciliate 18s, a discrete Gamma distribution was used to model evolutionary rate differences among sites (5 categories (+G, parameter = 0.2926)). The rate variation model allowed for some sites to be evolutionarily invariable ([+I], 28.74% sites). The analysis involved 167 nucleotide sequences and there were a total of 1472 positions in the final dataset. For ciliate 28s, a discrete Gamma distribution was used to model evolutionary rate differences among sites (5 categories (+G, parameter = 0.5083)). The rate variation model allowed for some sites to be evolutionarily invariable ([+I], 27.50% sites). This analysis involved 34 nucleotide sequences. There were a total of 600 positions in the final dataset.

### 3. Results

#### 3.1.1. Quantitative assessment of MZP community Abundance and biomass

The spring MZP bloom was defined by a sharp increase in biomass starting between 71 – 79 Julian days (JD) with an initial MZP abundance and biomass of 450 cells L<sup>-1</sup> and 1,9 µg C L<sup>-1</sup> respectively, reaching peak values of 27160 cells L<sup>-1</sup> and 126 µg C L<sup>-1</sup> on JD 120 (figure 4a, b) Overall, this represents a 66-fold increase in biomass from low to peak.

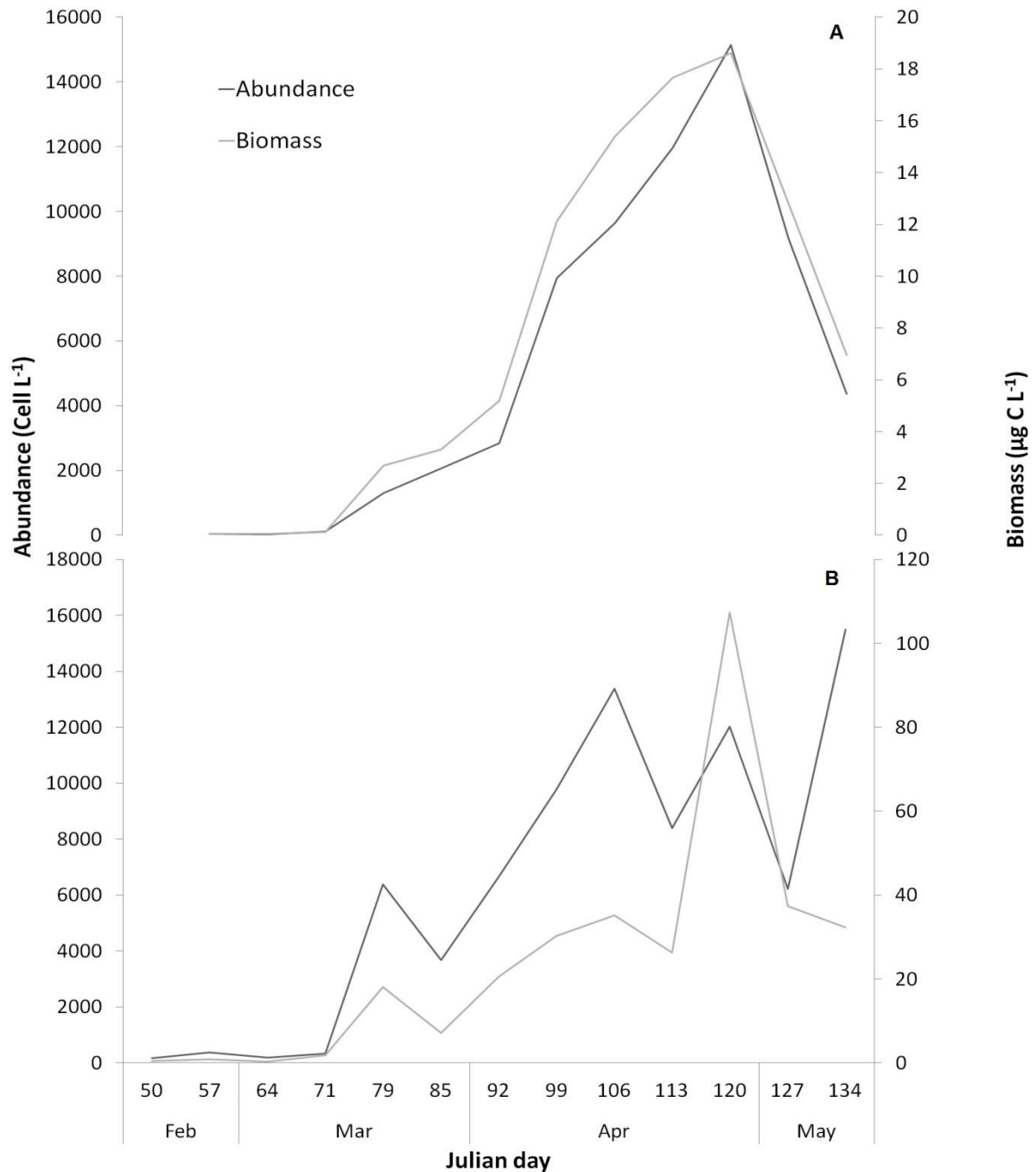


**Figure 4:** Dinoflagellate (a) and ciliate (b) abundance (Cell L<sup>-1</sup>) and biomass (µg C L<sup>-1</sup>) during a 84 day sampling series in spring 2019 with 13 sampling dates (Julian days; Month).

The relative abundance of ciliates versus dinoflagellates varied throughout the sampling period with ciliate taxa dominating the early spring season while relative dinoflagellate abundance increased in the later spring period (figure 5a). The highest relative abundance observed for dinoflagellates was approximately 60 percent in JD 127 while the highest relative abundance for ciliates was 100 percent on JD 50. The relative biomass of ciliates was higher than dinoflagellates throughout the sampling period although an increase of relative dinoflagellate biomass was observed in later spring (figure 5b) when dinoflagellates made-up approximately 40 percent of the total biomass.

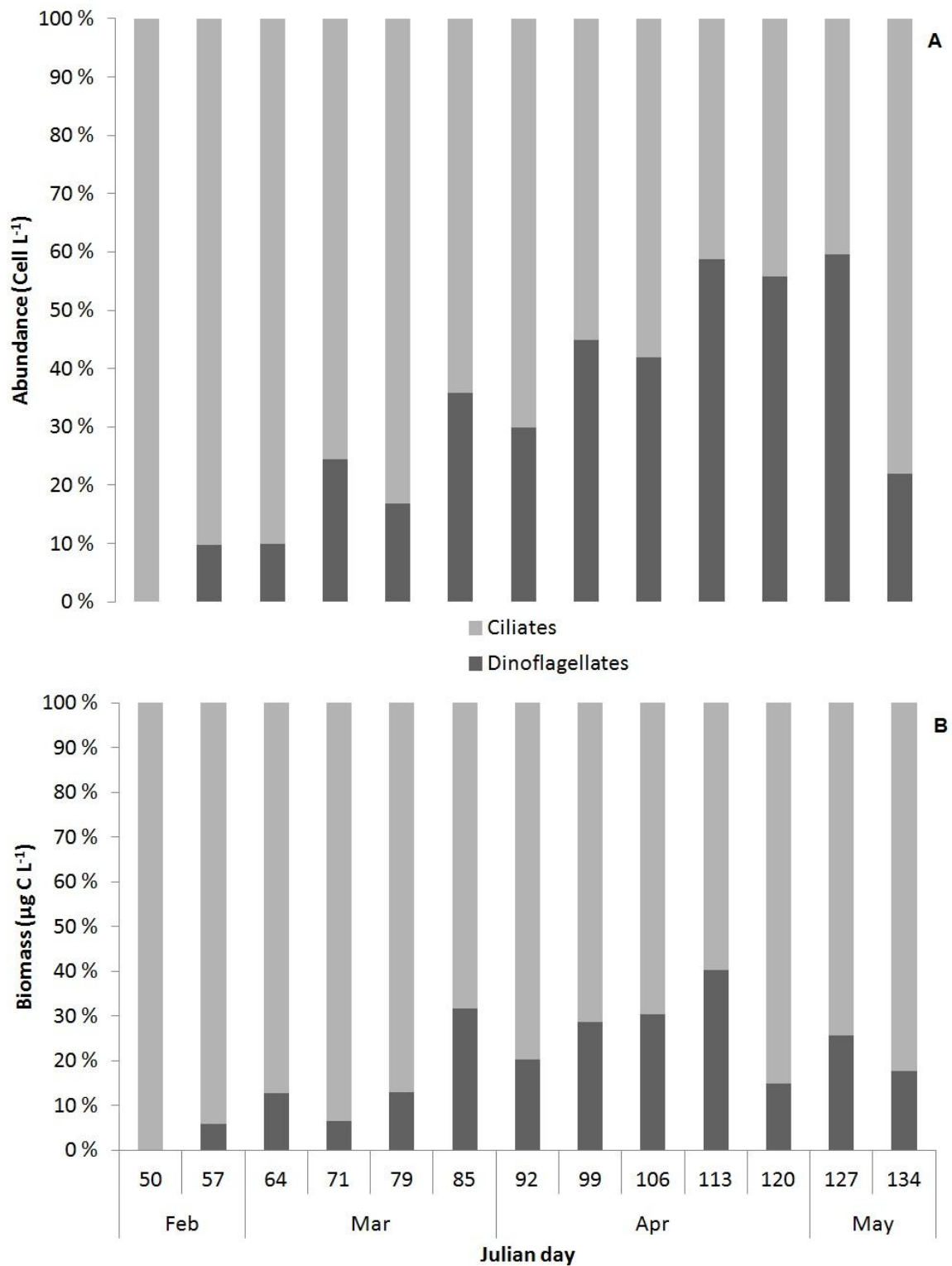


**Figure 5:** Relative abundance (a) and biomass (b) of ciliates (light gray) and dinoflagellates (dark gray) during a 84 day sampling series in spring 2019 with 13 samples (Julian days; Month).

Variation in size fraction distribution was observed for both dinoflagellates and ciliates throughout the sampling period.

In dinoflagellates, size fractions 25-50  $\mu\text{m}$  and >50  $\mu\text{m}$  dominated the first sampling events until JD 92, where cells belonging to the smallest fraction, <25  $\mu\text{m}$  were first observed (figure

6a). At JD 120, a maximum relative abundance for  $<25\ \mu\text{m}$  was observed with more than half of the dinoflagellate cells belonging to this size fraction. In ciliates, the variation in relative abundance was the largest for the size fraction  $>50\ \mu\text{m}$ . Initially not being observed on JD 50, this size fraction comprised of more than 60 percent of the ciliate cells observed on JD 120 (figure 6b). When it comes to the relative biomass of dinoflagellates, size fraction  $25 - 50\ \mu\text{m}$  was observed to be the largest in all sampling dates except JDs 57 and 64 where the  $<25\ \mu\text{m}$  made up an equal or larger part.

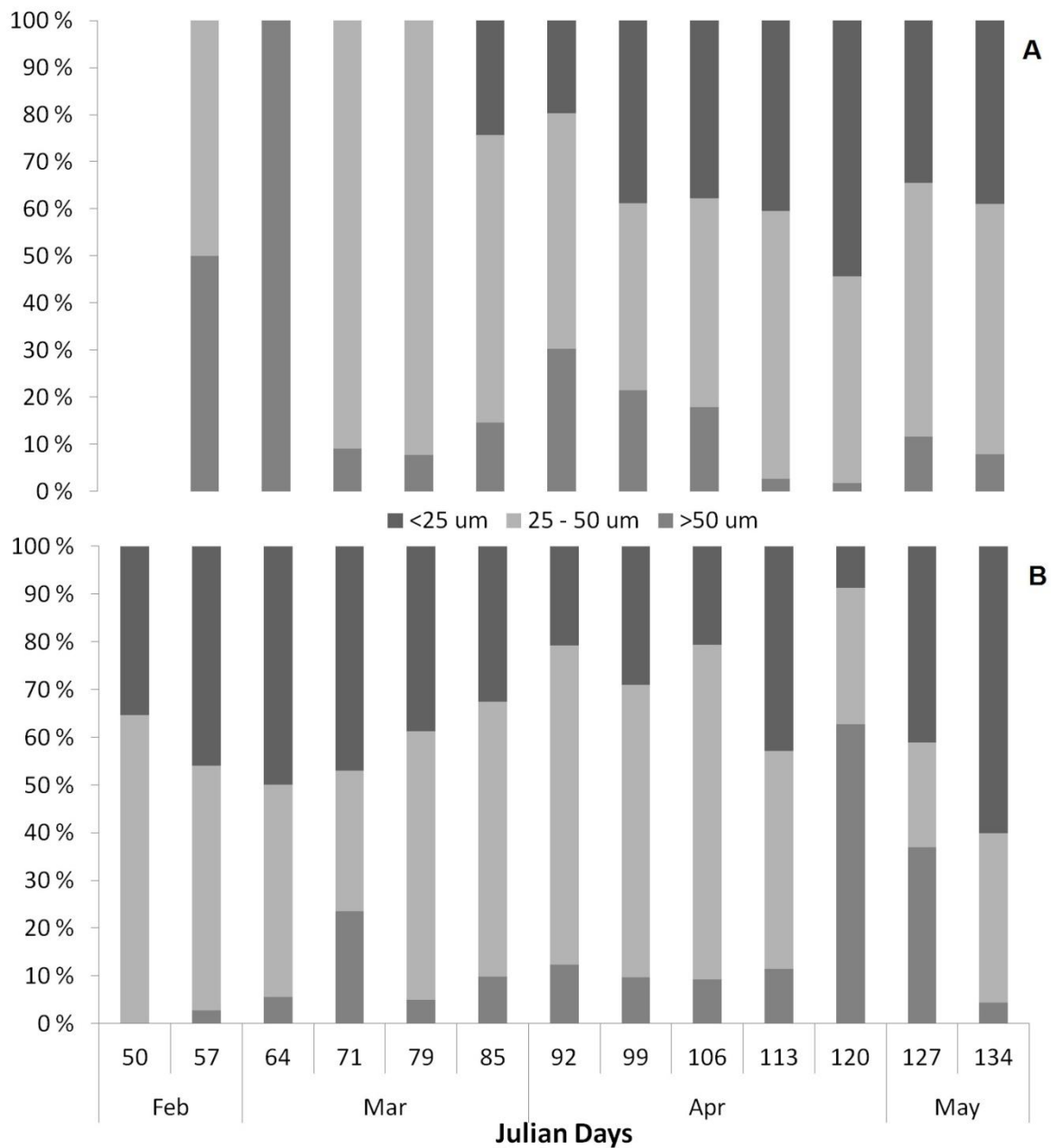


**Figure 6:** Relative abundance of three size classes,  $<25\ \mu\text{m}$ ,  $25-50\ \mu\text{m}$  and  $>50\ \mu\text{m}$ , of dinoflagellates (a) and ciliates (b) during a 84 day sampling series (Julian days; Month) in spring 2019.

In these days the largest size fraction,  $>50\ \mu\text{m}$ , had the largest biomass (figure 7a). , The highest relative abundance for size class  $<25\ \mu\text{m}$  was seen on JD 120, making up approximately 55 percent of the total abundance(figure 7a). The dominant size class for ciliates was  $>50\ \mu\text{m}$  with an increasing relative biomass from the start of the sampling series to a relative biomass above 90 percent exhibited at JDs 120 and 127 (7b). Size class  $<25\ \mu\text{m}$  has a low relative biomass throughout the spring season while size class  $25\text{-}50\ \mu\text{m}$  dominated the early spring season in addition to the last sample (JD 134).

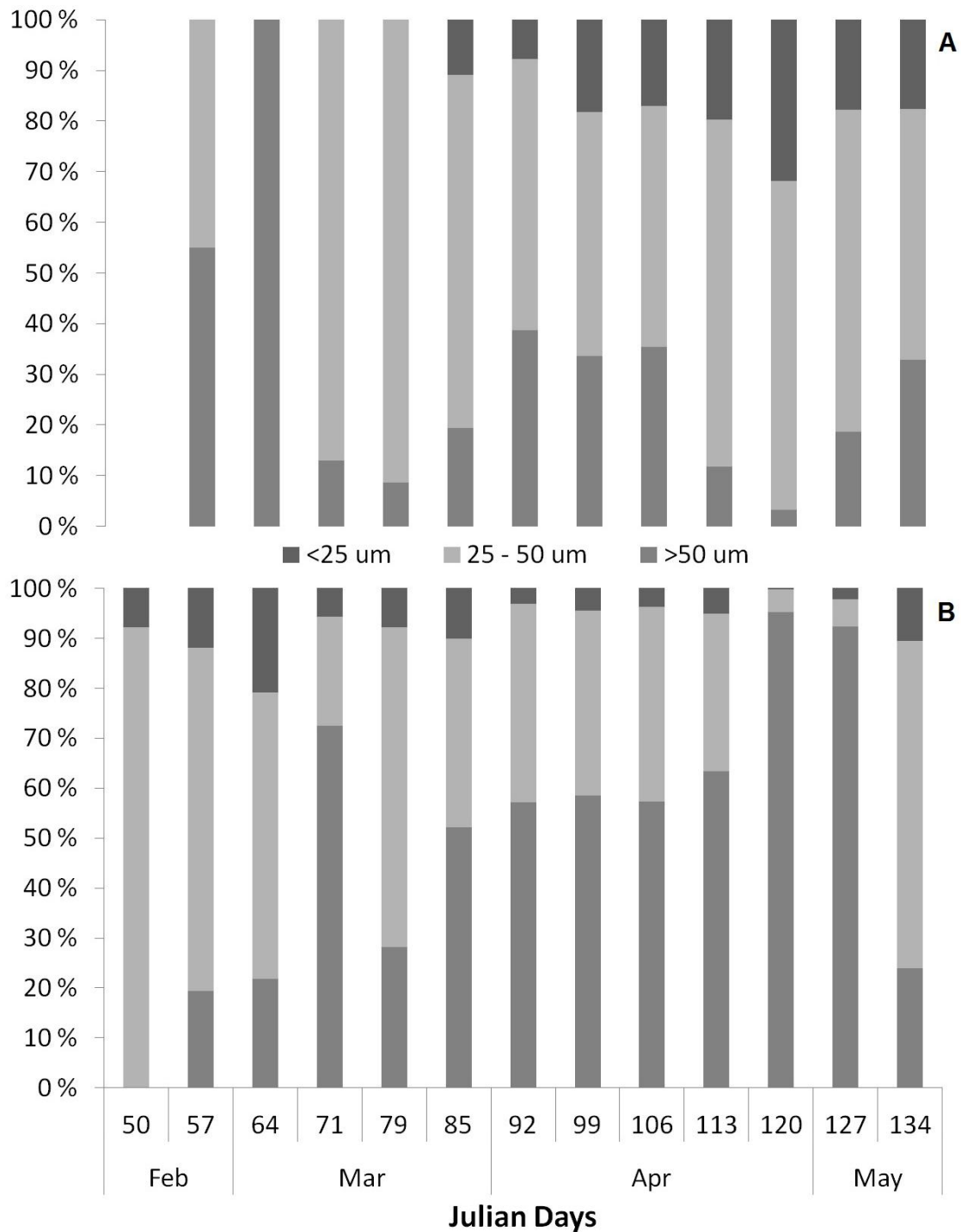
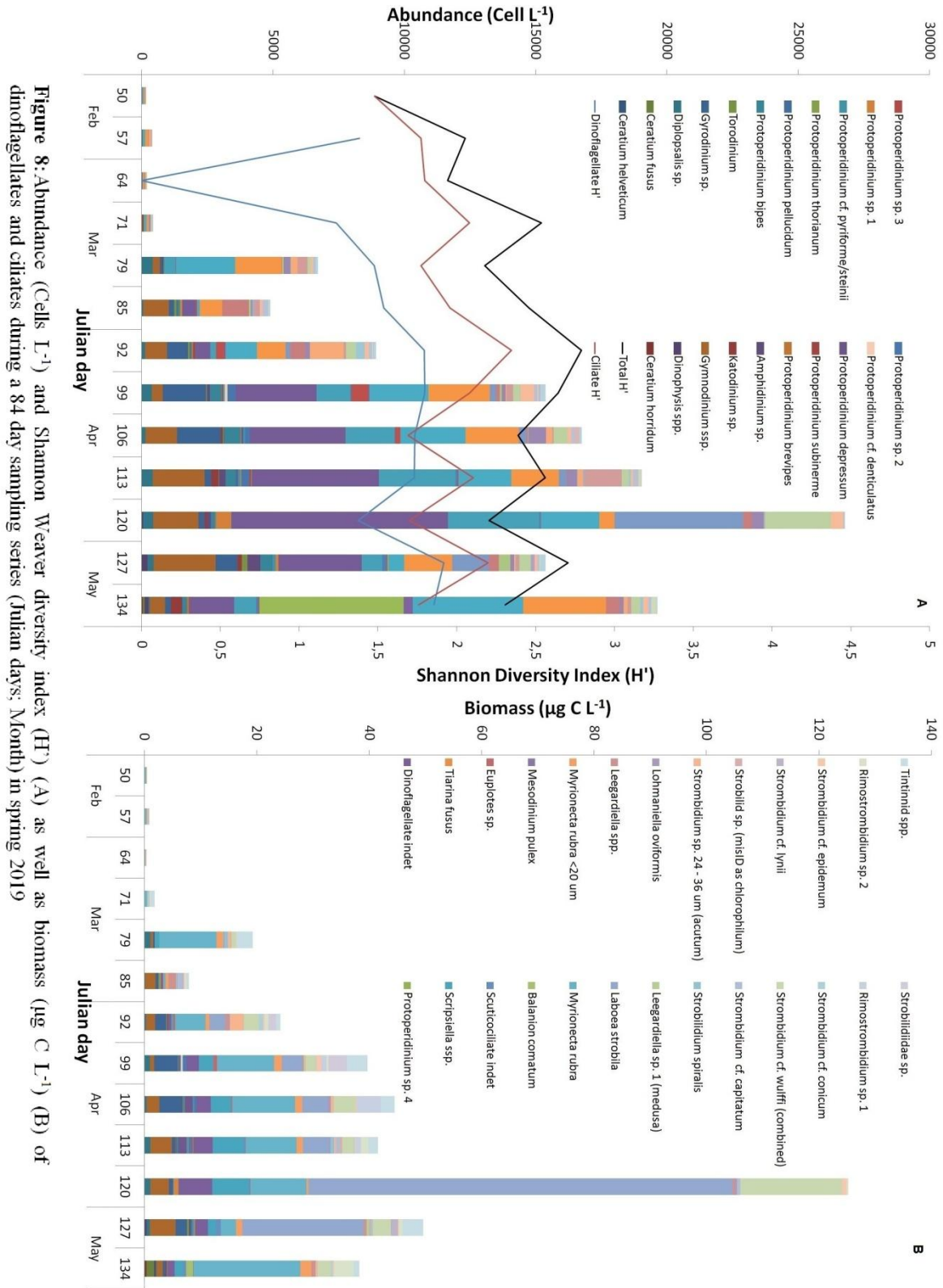


**Figure 7:** Relative biomass of three size classes, <25μm, 25-50 μm and >50 μm of dinoflagellates (a) and ciliates (b) during a 84 day sampling series (Julian days; Month) in spring 2019.

The most abundant dinoflagellate taxa observed throughout the sampling period were *Scrippsiella spp.* (9D) and *Gymnodinium spp.* (9E) in addition to indetermined dinoflagellates with totals of 11840, 10370 and 25700 cells L<sup>-1</sup> observed respectively (table 4; figure 8a). The highest abundances observed in a sample were undetermined dinoflagellates on JD 120 with 8220 Cells L<sup>-1</sup> and *Strombidium sp.* “26 μm” (figure 9k) with 6260 Cells L<sup>-1</sup> observed on JD

106. For ciliates, the most abundant taxa observed were both size classes of *Mesodinium rubrum* (<20, >20  $\mu\text{m}$ ; figure 9J,) in addition to *Strombidium sp.* “26  $\mu\text{m}$ ”. The numbers observed were 15770, 17560 and 12860 cells  $\text{L}^{-1}$  respectively (table 1; figure 5a).

In terms of biomass, the dominant taxa were *Scrippsiella spp.* (figure 9D), *Gymnodinium spp.* (figure 9E) in addition to indetermined dinoflagellates with a total of 22.2, 19.9 and 18.5  $\mu\text{g C L}^{-1}$  observed respectively (table 4; figure 8B). The dominant species in terms of biomass for ciliates were *Laboea cf. strobila* (figure 7f), *Mesodinium cf. rubrum* and *Strombidium cf. wulffi* (figure 9I) with observed totals of 112.8, 79.2 and 35.3  $\mu\text{g C L}^{-1}$  respectively (table 4; figure 8B).



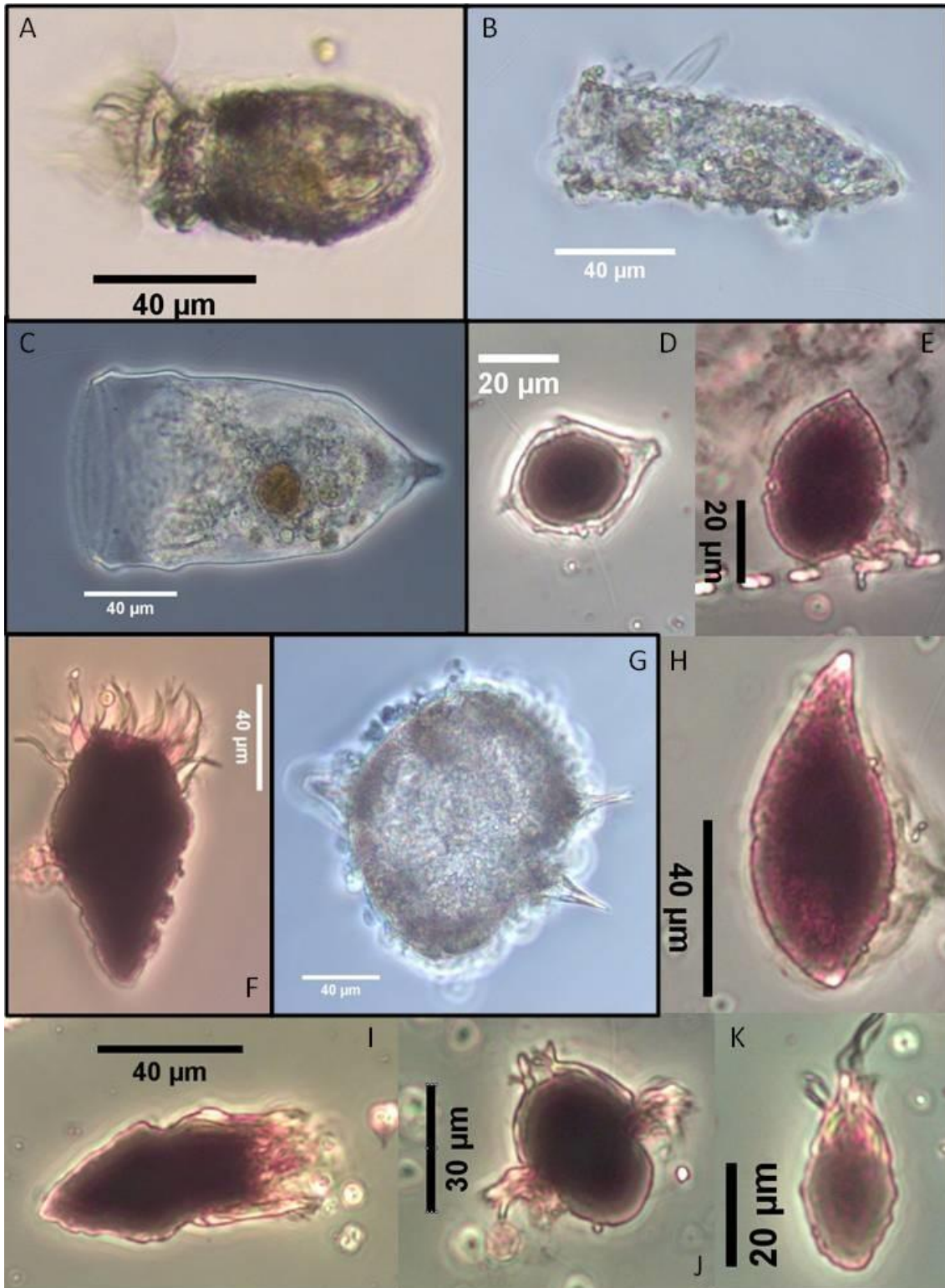


**Figure 8:** A selection of species from spring 2019 sampling series and 2018-2019 single cell isolation. Molecular data was obtained for the species marked with a black border. Undetermined tintinnid ciliate (A), *Tintinnopsis* sp. (B), Undetermined tintinnid ciliate (C), *Scrippsiella* cf. *trochoidea* (D), *Gymnodinium* cf. *helveticum* (E), *Laboea* cf. *strobila* (F), *Protoperidinium* sp. (G), *Gyrodinium* cf. *spirale* (H), *Strombidium* cf. *wulffi* (I), *Mesodinium* cf. *rubrum* (J), *Strombidium* sp. “20 – 32 µm” (K). Live (A-C, G) and Lugol-fixed (D-F,H-K) specimens. Photos taken with Leica DM IRB Inverted microscope (20x objective).

### 3.1.2. Diversity

During the spring sampling period a total of 50 taxa were identified, 23 being dinoflagellate taxa and 27 ciliate taxa (table 4). Out of the taxa identified, the genera *Protoperidinium* and *Strombidium* were the most diverse with 12 and 9 morphologically different species observed respectively.

Shannon Weaver diversity index (H') for each sampling showed a variable diversity from sample to sample with an overall increasing trend towards the abundance and biomass maxima (figure 8A). The lowest total H' was seen on JD 50 with a value of 1.47 and the highest total H' on JD 92 with a value of 2.79. Maximum H' values for ciliates and dinoflagellates were 2.34 (JD 92) and 1.91 (JD 120) respectively.

**Table 4:** List of ciliates and dinoflagellates identified from the sampling series including size category, maximum abundance, peak timing, mean biovolume, and mean carbon content of each taxon.

Taxa	Size category (µm)	Maximum Abundance (Cell L <sup>-1</sup> )	Maximum Biomass (µg C L <sup>-1</sup> )	Bloom peak (Julian day)	Biovolume (µm <sup>3</sup> Cell L <sup>-1</sup> )	Carbon (pg C L <sup>-1</sup> )
<i>Indet dinoflagellate</i>	<25	8220	5.92	120	4310.38	4310.38
Order Gonyaulacales						
<i>Ceratium cf. helveticum</i>	>50	20	0.02	120	6808.55	1047.33
<i>Ceratium cf. horridum</i>	>50	40	0.39	134	106180.67	9934.47
<i>Ceratium cf. fusus</i>	>50	80	1.35	132	203270.58	16909.33
Order Dinophyceae						
<i>Dinophysis spp.</i>	25 - 50	220	0.39	127	13249.27	1806.71
Order Gymnodiniales						
<i>Torodinium sp.</i>	>50	220	0.26	127	11477.84	1606.34
<i>Gyrodinium sp.</i>	>50	1660	4.53	99	18885.52	2415.25
<i>Gymnodinium sp.</i>	25 - 50	2360	4.00	127	9515.92	1377.73
Order Tovelliales						
<i>Katodinium sp.</i>	25 - 50	420	0.15	132	1880.25	365.08
Order Amphidinales						
<i>Amphidinium sp.</i>	25 - 50	480	0.35	127	3161.80	558.80
Order Peridinales						
<i>Scrippsiella spp.</i>	25 - 50	3480	6.54	120	13911.01	1880.28
<i>Diplopsalis sp.</i>	25 - 50	420	1.08	79	20427.76	2575.63
<i>Protoperidinium cf. bipes</i>	25 - 50	620	0.32	106	2967.08	530.45
<i>Protoperidinium cf. brevipes</i>	25 - 50	60	0.05	132	5948.46	937.67
<i>Protoperidinium cf. pellucidum</i>	25 - 50	60	0.14	113	19366.28	2465.49
<i>Protoperidinium cf. subinermis</i>	25 - 50	80	0.27	92	28831.08	3415.38
<i>Protoperidinium cf. thorianum</i>	25 - 50	20	0.09	85	41006.01	4557.59
<i>Protoperidinium cf. depressum</i>	>50	40	1.40	106-	498181.75	35234.99

				113			
<i>Protopteridinium cf. pyriforme</i>	25 - 50	120	0.34	127	23644.55	2903.34	
<i>Protopteridinium cf. denticulatus</i>	25 - 50	120	0.34	99	23285.25	2867.16	
<i>Protopteridinium sp. 1</i>	25 - 50	580	0.88	120	10725.06	1519.53	
<i>Protopteridinium sp. 2</i>	25 - 50	300	0.67	113	17204.39	2237.70	
<i>Protopteridinium sp. 3</i>	25 - 50	80	0.12	113	11229.44	1577.81	
<i>Protopteridinium sp. 4</i>	25 - 50	20	0.04	113	19373.73	2466.27	
Order Prorodontida							
<i>Tiarina cf. fusus</i>	25 - 50	10	0.04	50	24543.69	4663.30	
<i>Balanion cf. comatum</i>	<25	5500	1.23	134	1177.15	223.66	
Class Oligohymenophorea							
<i>Scuticociliate indet</i>	25 - 50	160	0.79	127	26243.05	4986.17	
Order Euplotida							
<i>Euplotes sp.</i>	25 - 50	660	0.64	99	5128.26	974.37	
Order Cyclotrichiida							
<i>Mesodinium cf. pulex</i>	<25	340	0.14	134	2181.96	414.57	
<i>Mesodinium cf. rubrum</i>	25 - 50	4200	18.93	134	23726.59	4508.05	
<i>Mesodinium cf. rubrum</i>	<25	3160	1.91	134	3181.82	604.54	
Order Oligotrichiida							
<i>Laboea cf. strobila</i>	>50	4900	75.50	120	81100.57	15409.10	
<i>Strombidium cf. capitatum</i>	>50	60	0.92	85	81212.10	15430.29	
<i>Strombidium cf. conicum</i>	25 - 50	340	0.79	92	12235.08	2324.66	
<i>Strombidium cf. epidemum</i>	25 - 50	520	0.81	99	8263.85	1570.13	
<i>Strombidium cf. lynii</i>	>50	140	1.29	127	48714.06	9255.67	
<i>Strombidium cf. wulffi</i>	>50	2520	18.14	120	37889.93	7199.08	
<i>Strombidium sp. 26 µm</i>	25 - 50	6260	5.08	120	4274.63	812.18	
<i>Strombidium sp. 31 µm</i>	25 - 50	1300	2.41	92	9795.03	1861.05	
<i>Strombidium sp. 100 µm</i>	>50	220	1.87	85	44923.37	8535.44	
<i>Strobilidium cf. spiralis</i>	>50	20	0.67	79	473799.07	33816.23	
Order Choreotrichiida							
<i>Leegardiella spp.</i>	25 - 50	1000	1.32	85	6991.29	1328.34	
<i>Leegardiella sp. 1</i>	<25	440	0.58	127	2699.40	512.88	
<i>Lohmaniella cf. oviformis</i>	<25	680	0.40	106	3139.05	596.41	
<i>Strobilidium sp. 1</i>	<25	1420	0.47	113	1755.13	333.47	
<i>Strobilidium sp. 2</i>	>50	80	3.29	134	86782.09	16488.59	
<i>Rimostrombidium sp. 1</i>	>50	180	4.32	106	126339.60	24004.52	
<i>Rimostrombidium sp. 2</i>	>50	200	3.44	134	90701.67	17233.31	
<i>Stenosemella sp. 1</i>	>50	80	2.10	92	52850.40	10041.57	
<i>Tintinnopsis sp.</i>	>50	120	3.99	99	70080.26	13315.25	
<i>Tintinnid sp. 1</i>	25 - 50	100	0.43	134	23141.58	4396.90	
<i>Tintinnid indet</i>	>50	90	7.01	79	369185.72	70145.28	

## **3.2. Molecular analysis**

### **3.2.1. Protocol development**

Of the different tests of the single-cell isolation method, a protocol with the use of MQ-water and PCR master mix for cell isolation was proven to be the most reliable. To limit osmotic stress, single cells were picked along with sample water for photography. Especially for aloricate ciliates which tend to be fragile when it comes to osmotic changes and changes in temperature, a quick procedure is key to successfully isolate the cells. The photography step of the isolation process proved to be difficult due to having to switch back and forth to the reverse microscope for this step. Single-cell isolation showed that some taxa were more fragile and therefore more difficult to isolate than others. Aloricate ciliates and especially oligotrich ciliates proved to be the most difficult to isolate as the single cells would burst with little stress applied, the critical step being picking and photography of the cells. To circumvent the difficult steps of the protocol, fragile cells were fixed with Lugol before a picture was taken. This method was satisfactory when abundances were high enough to isolate and identify several individual from the same species at once.

The method of washing whole Lugol-fixed samples with autoclaved seawater yielded one positive result in Gel but no viable sequences. Single-cell isolation with thiosulphate washing yielded one positive result in Gel and one sequence. A BLAST query for the sequence determined low sequence quality due to low query cover.

Four different primer sets were tested to see which would work. Although some positive Gel results would be retrieved from the primer pair 18scom F1/R1 (table 1), sequencing provided no further results. The combination of the primers F1/18scom R1 (table 1) which aligned well with existing MZP sequences did not provide any positive results. The primer pair 1F/1528R yielded the best result out of all primers used (table 1). Out of the 31 samples that were run with a nested PCR, 12 positive results were obtained. Nested PCR gel results showed single bands and only the 28s gene was successfully amplified.

### **3.2.2. Single cell isolation**

A total of 456 samples for PCR were isolated from February 2018 to May 2019. 291 were isolated from collected natural seawater samples, 66 from MZP cultures and 99 samples were isolated from Lugol-fixed natural seawater samples. In total, single cells from 15 different

taxa were isolated in the autumn 2018 season and 17 different taxa in the spring season (2018 and 2019). The most diverse groups were tintinnids with 15 morphologically different taxa isolated and the dinoflagellate genus *Protooperidinium* with 6 morphologically different taxa isolated.

### 3.2.3. BLAST identification

BLAST queries revealed a species level match for 11 samples and matches at genus level for 7 samples (table 5; Altschul et al. 1990). 4 samples showed good matches with two or more taxa and 2 samples had low identity matches with non MZP taxa. 1 sample had a high identity match with a non MZP taxa. Samples 73, 77 and 82 were identified as *Protooperidinium depressum*, sample 82 was identified as *Protooperidinium conicum*, sample 59 was identified as *Tintinnopsis cylindrica*, and samples 100, 101, 102, 105, 106, 98 were identified as *Laboea strobila*. Sample 75 showed high identity matches with three different tintinnid taxa, *Cymatocylis calyciformis*, *Ptychocylis minor*, and *Favella sp.* Sample 4 had high identity matches with *Codonellopsis mobilis*, *Stenosemella ventricosa* and *Stenosemella pacifica*. Sample 3 had high identity matches with *Stenosemella pacifica*, *Codonellopsis gaussi*, *Codonella apicata*, and *Laackmanniella prolongata*. Sample 2 showed high identity matches with two *Stenosemella pacifica* sequences.

**Table 5:** BLAST query results with morphological identity, picture reference, BLAST identify with accession number, query cover and identity (Altschul et al. 1990).

Sample (no.)	Morphological ID	Picture ref.	BLAST ID	Accession No.	Query cover (%)	Identity (%)
76	<i>Protoperidinium</i> sp.1		<i>Chaetoceros debilis</i>	<a href="#">MG972245.1</a>	100	99,88
			<i>Uncultured Alveolate</i>	<a href="#">LC371035.1</a>	100	99,90
73	<i>Protoperidinium</i> sp. 1		<i>Protoperidinium depressum</i>	<a href="#">AB255834.1</a>	98	99,70
77	<i>Protoperidinium</i> sp. 1	Figure 9G	<i>Protoperidinium depressum</i>	<a href="#">AB255834.1</a>	99	99,40
81	<i>Protoperidinium</i> sp. 2		<i>Protoperidinium conicum</i>	<a href="#">AB181883.1</a>	99	93,77
82	<i>Protoperidinium</i> sp. 1		<i>Protoperidinium depressum</i>	<a href="#">AB255834.1</a>	98	99,64
62	<i>Tintinnopsis</i> sp.		<i>Tintinnopsis</i> sp.	<a href="#">MF460775.1</a>	100	99,75
65	<i>Tintinnopsis</i> sp.		<i>Tintinnopsis</i> sp.	<a href="#">MF460775.1</a>	100	100
67	<i>Tintinnopsis</i> sp.		<i>Tintinnopsis</i> sp.	<a href="#">JX178872.1</a>	100	100
69	<i>Tintinnopsis</i> sp.		<i>Tintinnopsis</i> sp.	<a href="#">JX178872.1</a>	100	100
71	<i>Tintinnopsis</i> sp.	Figure 9B	<i>Tintinnopsis</i> sp.	<a href="#">JX178872.1</a>	100	99,94
72	<i>Tintinnopsis</i> sp.		<i>Tintinnopsis</i> sp.	<a href="#">JX178872.1</a>	100	99,88
83	<i>Tintinnopsis</i> sp.		<i>Tintinnopsis</i> sp.	<a href="#">JX178872.1</a>	100	100
56	<i>Tintinnopsis</i> sp.		<i>Uncultured tintinnid ciliate</i>	<a href="#">KX158693.1</a>	100	99,66
59	Undetermined tintinnid		<i>Tintinnopsis cylindrica</i>	<a href="#">KU715790.1</a>	100	99,32
100	<i>Laboea cf. strobila</i>		<i>Laboea strobila</i>	<a href="#">KU715780.1</a>	57	99,66
101	<i>Laboea cf. strobila</i>		<i>Laboea strobila</i>	<a href="#">KU715780.1</a>	72	99,83
102	<i>Laboea cf. strobila</i>		<i>Laboea strobila</i>	<a href="#">KU715780.1</a>	100	99,66
105	<i>Laboea cf. strobila</i>		<i>Laboea strobila</i>	<a href="#">KU715780.1</a>	100	99,50
106	<i>Laboea cf. strobila</i>		<i>Laboea strobila</i>	<a href="#">KU715780.1</a>	72	99,16
128	<i>Laboea cf. strobila</i>		<i>Ciona intestinalis</i>	<a href="#">AF212177.1</a>	97	83,27
54			<i>Asterocladon lobatum</i>	<a href="#">AJ229136.2</a>	63	85,57
75	Undetermined tintinnid		<i>Cymatocylis calyciformis</i>	<a href="#">JQ924046.1</a>	100	98,98
			<i>Ptychocylis minor</i>	<a href="#">KY290321.1</a>	98	99,51
			<i>Favella</i> sp.	<a href="#">JX178773.1</a>	100	98,08
98	<i>Laboea cf. strobila</i>		<i>Laboea strobila</i>	<a href="#">AF399153.1</a>	100	99,94
			<i>Laboea strobila</i>	<a href="#">AF399152.1</a>	100	99,88
4	<i>Stenosemella</i> sp. 1		<i>Codonellopsis mobilis</i>	<a href="#">MK799838.1</a>	100	100
			<i>Stenosemella ventricosa</i>	<a href="#">KU715764.1</a>	100	100
			<i>Stenosemella pacifica</i>	<a href="#">JN831794.1</a>	100	100
3	<i>Stenosemella</i> sp. 1	Figure 9A	<i>Stenosemella pacifica</i>	<a href="#">JN831794.1</a>	100	99,80
			<i>Laackmanniella</i>	<a href="#">JQ924056.1</a>	100	98,63

---

		<i>prolongata</i>		
		<i>Codonellopsis gaussi</i>	<a href="#">JQ924053.1</a>	100 98,43
		<i>Codonella apicata</i>	<a href="#">EU399531.1</a>	100 98,37
<b>2</b>	<i>Stenosemella sp. 1</i>	<i>Stenosemella pacifica</i>	<a href="#">JN831794.1</a>	100 89,11
		<i>Stenosemella pacifica</i>	<a href="#">JN831790.1</a>	98 89,11a

---

### 3.2.4. Phylogenetics

Alignments determined 14 sequences to be suitable for use in further analysis to determine the species identity. Out of the 14 sequences 6 were 28S ciliate samples, additional 6 were 18S ciliate samples and the remaining 3 were dinoflagellate 18s samples. A 28s phylogeny was inferred from six ciliate samples in addition to reference sequences available from Genbank (figure 10). Four samples of isolated *Laboea cf. strobila* were resolved as outgroups similarly with two *L. strobila* sequences from Genbank. Two samples of isolated tintinnids formed clades with *Tintinnopsis cylindrica* and sequences marked as unidentified tintinnid ciliate respectively.

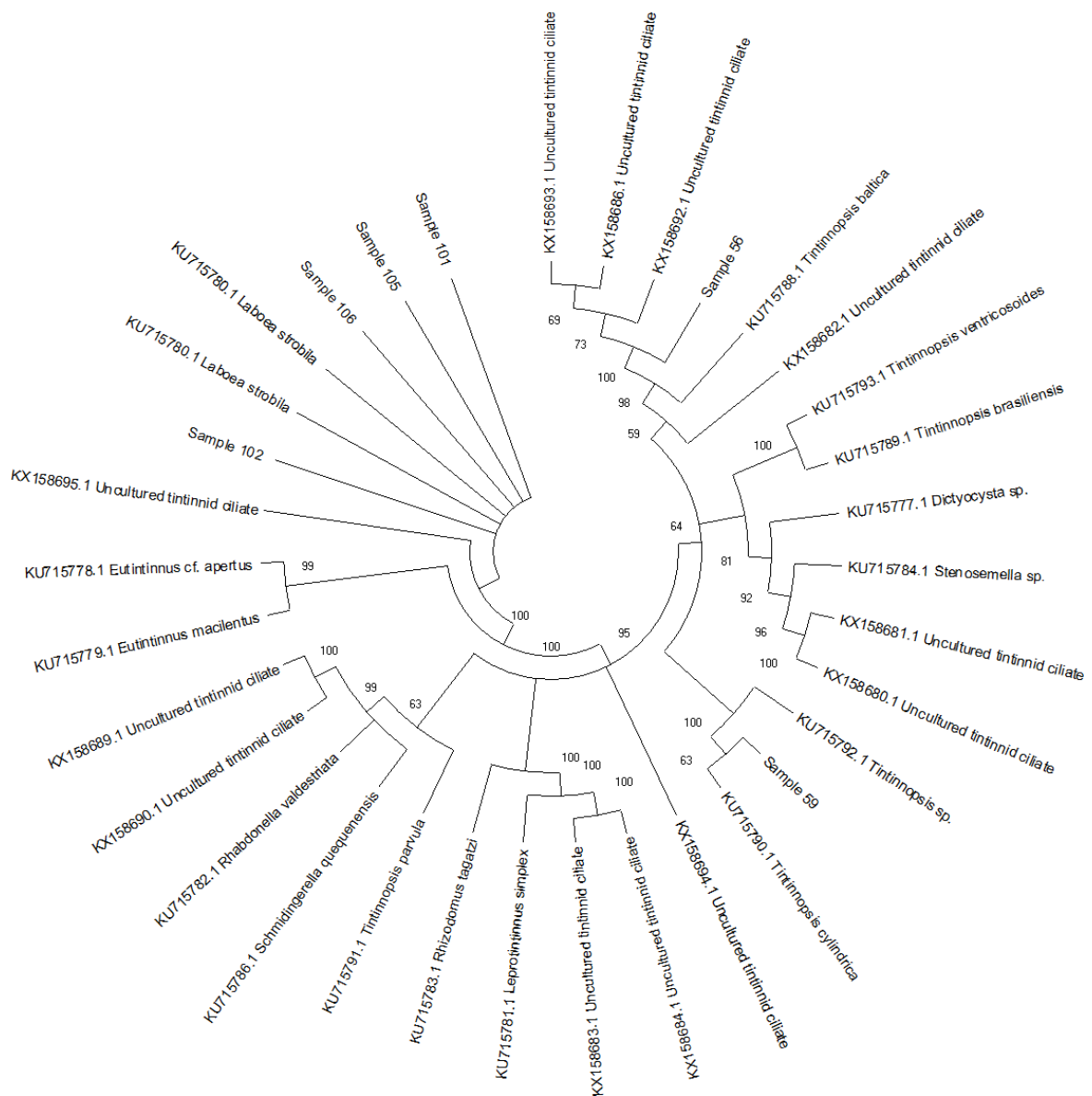


**Figure 9:** 28 s phylogram (Maximum Likelihood, 500 bootstraps, support threshold) comprising of ciliate single cells isolation sample sequences (denoted as sample followed by a two or three digit number) in addition to sequences downloaded from Genbank. Branch values are bootstrap percentages.

For 18s two phylogenies were inferred with ciliates and dinoflagellate sequences. One tree comprised of 6 ciliate samples along with ciliate reference sequences available from Genbank (figure 11). Sample 98 isolated as *L. cf. strobila* formed a clade with tontonid ciliates from the genus *Spirotontonia*. Sample 75 (figure 9C), an indetermined tintinnid formed a clade with *Cymatocylis*, *Metacylis* and *Rhabdonella* sequences in addition to indetermined tintinnid sequences. Samples 71, 72 and 83 isolated as *Tintinnopsis sp.* (figure 9B) formed a clade with reference *Tintinnopsis sp.* sequences in addition to indetermined tintinnid sequences. Sample 3 (figure 9A), an indetermined tintinnid sample formed a clade with *Codonellopsis*, *Tintinnopsis*, *Stenosemella* and *Laackmanniella* tintinnid in addition to indetermined tintinnid sequences.





## 4. Discussion

### 4.1. Microzooplankton community assessment during spring 2019

Microzooplankton cell counts using classical microscopy help to provide an understanding of abundance, biomass and diversity patterns of MZP e.g. during spring bloom events. From the microscopic MZP enumeration, bloom dynamics and duration could be observed both for heterotrophic dinoflagellates and ciliate species.

From the abundance and biomass data of ciliates and heterotrophic dinoflagellates it became obvious that ciliates dominated in early spring while heterotrophic dinoflagellates increased in late spring. Löder et al. (2012) showed that heterotrophic dinoflagellates differ from ciliates in terms of succession pattern and growth during spring blooms with ciliates appearing earlier in larger numbers and with faster growth responses. This is evident when looking at specific ciliate taxa such as *Mesodinium* and *Laboea* with especially *Laboea* displaying a rapid increase in abundance and biomass over a short period of time (Montagnes, 1996). One of the reasons for the succession pattern of ciliates and dinoflagellates is the prey size preference (Calbet & Alcaraz, 2009). While ciliates generally ingest smaller prey, dinoflagellates are known to have wider size range when it comes to prey organisms. While it is thought that ciliates generally prefer smaller prey, it has been demonstrated that some species may prey on large chain-forming diatoms and dinoflagellates (Aberle et al. 2007). Furthermore, ciliates and dinoflagellates differ in their ability to withstand starvation with dinoflagellates being able to survive for longer periods than ciliates (Löder et al. 2012). Another reason for the succession of ciliates and dinoflagellates is the increased predation by mesozooplankton in spring although it is argued that predation regulate abundance rather than occurrence of MZP (Löder et al. 2012; Smetacek, 1981). Temperature changes may also be a factor affecting the MZP community. Temperature affects metabolism in zooplankton and it is argued that changes in temperatures over time may affect the growth rates and timing of the MZP succession in spring (Aberle et al. 2007).

The abundance and biomass of ciliates and dinoflagellates found for spring MZP communities in this study is overall high compared to other studies on MZP from Trondheimsfjorden and the North Sea in spring (Tokle, 1999; Yang et al. 2004; Löder et al. 2012). An explanation for the differences in abundance and biomass is the evident patchiness in MZP distribution which can lead to large variation in monitoring data. (Montagnes 1996; Yang et al. 2004). Rapid

increase in growth rate as a response to available prey can also explain a discrepancy in abundance between studies (Montagnes, 1996) as well as annual variation. The high abundance of *L. strobila* can help shedding light on the impact of a single species during a spring bloom period and also highlights its bloom forming potential.

Size fraction of ciliates and heterotrophic dinoflagellates help to indicate functional roles of the MZP community (Tokle, 1999). When it comes to ciliates, the smallest size fraction <25 µm is considered to be preying on bacteria and picoplankton while the size fraction 20 - 50 µm is considered to be preying on nanoplankton (Tokle, 1999). The largest fraction >50 µm is thought to be preying on nano and microplankton. Whereas the smallest size fraction (<25 µm) of both ciliates and heterotrophic dinoflagellates accounts for a large abundance, the relative biomass contribution of this size fraction was low. Differences in abundance and biomass proved to be smaller in the two larger size fractions due to the larger biovolumes. Shifts in abundance of the different size fractions can be explained by increased predation on MZP. The strong shifts in relative abundance of the largest size fraction (> 50 µm) of ciliates might be explained by predation pressure since one of the main predators, copepods, generally prefer larger ciliates in the size class >50 µm as prey (Tokle, 1999). When it comes to predation on dinoflagellates and ciliates by mesozooplankton there are evident differences in terms of protection against predators. While aloricate ciliates have shown to have higher abundances and biomass than their loricate counterparts they are also likely to be more prone to predation due to lacking a rigid cell structure. This is also evident for thecate versus atehcate dinoflagellates which share the same differences in cell structures.

The diversity of MZP was found to be low but also comparable to other studies. Löder et al. (2012) found a total of 105 MZP taxa occurring during spring, doubling the amount of species observed in this project. Of the 105 taxa, 56 were dinoflagellate and 49 were ciliates. With a total of 27 morphological species distinguished, the diversity of ciliates was higher than in a previous study in Trondheimsfjorden for the same period (Tokle, 1999) but lower than in another monitoring study in the North Sea (Yang et al. 2014). The lower diversity of heterotrophic dinoflagellates observed in the present study with only 23 taxa identified in spring, can be explained by the seasonal patterns of dinoflagellates which usually appear later than ciliates (Löder et al. 2012). The seasonal patterns can also be explained by the life histories of some ciliate groups, which under low prey densities have a rapid mortality rate and an overall short lifespan (Montagnes, 1996). Ability to withstand starvation generally

differs between ciliates and dinoflagellates with the latter being able to remain present in the water column during periods of low prey densities (Löder et al. 2012).

In this study, several key species in the microzooplankton community could be determined. *Mesodinium* species of two size classes were observed throughout the spring sampling period and made up a major part of the MZP community both in terms of abundance and biomass. *Mesodinium* species such as *M. rubrum* are considered mixotrophic and play an important part of the ciliate community in spring and summer (Yang et al. 2012). Due to their phototrophic nature these species respond to changes in nutrients and light conditions and are considered as typical bloom forming species. The dinoflagellate genus *Protoperidinium* was the most diverse during the spring monitoring. This group of heterotrophic dinoflagellates exhibit a wide prey selection including diatoms, other dinoflagellates and even conspecifics (Jeong & Latz, 1994). The contribution of *Protoperidinium* grazing on diatoms is proven to be substantial with evidence of grazing suggested to surpass that of dominant mesozooplankton (Jeong et al. 2004). The ciliate *Laboea strobila* is another mixotrophic species which acts as both a heterotrophic grazer and an autotroph with the ability to perform photosynthesis with sequestered chloroplasts (Stoecker et al. 1987). Tokle (1999) observed an increase in ciliates in late March with a peak bloom consisting of primarily large ciliates (>50 µm) with *L. strobila* cells being dominant. *L. strobila* was shown to be a bloom forming species in this study and displayed the largest overall biomass in a late April peak.

The MZP community was monitored over a limited period of time during a single season. Year-to-year variations have been proved to be larger in fjords and coastal areas than in the open seas due to the larger variability of conditions affecting plankton blooms. Yang et al. (2014) demonstrates a large year to year variation in MZP biomass with one example of more than 100 percent increase in total biomass from one year to the next in the North Sea. Given the large variations showed it is evident that the numbers seen in this project would not be considered as anything else than a natural variation.

A coccolithophore bloom consisting of *Emiliana huxleyi* was observed in Trondheimsfjorden in 2018. The fact that MZP are known to graze very species-specific and to have a strong top-down control on coccolithophores (Widdicombe et al. 2002) might suggest that the MZP community composition in 2019 would differ from 2018. The overall trends in MZP observed during the spring bloom in 2019 corresponded well with previous studies such as Tokle

(1999) although a more intense monitoring would be beneficial to support these findings. In addition, phytoplankton data and abiotic measurements such as salinity, turbidity and nutrient content could help shedding light on the drivers of MZP dynamics in this study.

#### **4.2. Molecular species identification of microzooplankton**

Sequences for species identification were successfully obtained for both ciliates and heterotrophic dinoflagellates. Sequence identity, at least on family level, was confirmed from the open access reference libraries and for majority of the samples with expected taxa based on morphological identification as matches for the samples. 44 percent of samples found a match on species level while others matched with several closely related taxa. Overall BLAST queries showed that most samples were successful in terms of target DNA amplified.

Specific taxa identified by molecular methods in this project could be considered key MZP species during the spring season. The bloom forming oligotrich ciliate *L. strobila* which displayed a significant bloom peak (JD 120) in terms of biomass was well represented in the molecular results. The dinoflagellate genus *Protoberidinium*, which was found to be the most diverse taxon, was also represented with both 18 and 28s sequences. Although tintinnid abundance generally is low compared to oligotrich ciliates this groups can be diverse and play an important part of the MZP community in certain times of the year (Yang et al. 2004). In terms of molecular data gathered, tintinnids were the most diverse group. However, it is important to note that in terms of species covered there is a skew towards robust species such as loricate ciliates such as tintinnids and thecate dinoflagellates such as *Protoberidinium sp.* This bias may in part be due to the methodological challenges in single-cell isolation but can also be attributed to the abundance patterns in taxa present. Naturally, rare taxa would be more difficult to isolate due to the increase in search time in unfiltered seawater samples. Another reason for a bias in taxa represented is the possibility of short temporal windows for specific aloricate ciliates which may display rapid mortality rates and short life cycles (Montagnes, 1996).

*Laboea strobila* is a well-known oligotrich ciliate occurring all over the world although it is argued whether it is a cosmopolitan species or rather several species with discrete distribution ranges (Agatha et al. 2004). *L. strobila* is thought to be easily distinguishable from other oligotrichs due to its spiral cell structure. Later studies have, however, uncovered that the characteristic cell structure is also shared by the closely related species *Tontonia grandis*

(Agatha, 2004). This discovery may indicate that there has been some overrepresentation of *L. strobila* in monitoring studies due to possible misidentification using classical taxonomy approaches. This, in addition to the high peak numbers gathered in this project proves that *L. strobila* is an interesting target species for further molecular research. All *L. strobila* sequences obtained in this project were conclusively confirmed as *L. strobila* in BLAST results. The phylogeny also suggests that *L. strobila* is the correct identification due to the phylogenetic relationship to other tintinnids. *Protoperidinium* has been found to be the most divergent genus of heterotrophic dinoflagellates when it comes to rDNA (Gribble et al. 2007). This suggests that 18s and 28s markers can be effectively used to identify and distinguish these species. It was possible to identify three *Protoperidinium* isolates down to species level. In the phylogeny inferred, *Protoperidinium* was resolved to be paraphyletic which in turn may be supported by the high evolutionary divergence in this group (Gribble et al. 2007). Most of the sequences recovered in this project were isolated from tintinnid ciliates. Although the abundance and biomass of tintinnids is low in coastal waters, this group is present throughout the year in temperate oceans (Yang et al. 2014). Tintinnid genera such as *Tintinnopsis* and *Stenosemella* have proved to function as bioindicators to characterise water quality in a given environment (Feng et al. 2015). Establishing a reference library of local tintinnid species may be important in terms of biomonitoring and management of coastal waters.

In public reference libraries and earlier studies, 18s rDNA is the most commonly used genetic marker for the identification of protists. It is, however, not variable enough to resolve relationships between dinoflagellates and ciliates (Pawlowski et al. 2012). Regions of the 28s rDNA has been suggested for ciliates and used to successfully discriminate between dinoflagellate species (Pawlowski et al. 2012; Edvardsen et al. 2003). Identification of certain samples proved to be difficult with the 18s rDNA marker. 4 tintinnid samples were shown to match with close to full identity for several different reference taxa in BLAST queries. This suggests that interspecific variation for taxa such as *Stenosemella* and *Tintinnopsis* may be too low for species identification. Through the phylogenies inferred it was not possible to identify all samples down to a species level due to reference sequences with low taxonomic identification rank in addition to seemingly low interspecific variation in some taxa. A major part of the reference sequences available have a low degree of taxonomic identity. One example is the use of genus level such as *Tintinnopsis sp.* and also “uncultured tintinnid ciliate”. As many of these sequences with low taxonomic rank form close relations with the

samples obtained in this project, it underlines the importance of sequence metadata such as high-quality pictures for post hoc sample identification.

### **4.3. Methodology**

The development of working protocols for SCI and molecular methods was an important part of this project. A working protocol for molecular analyses of single-cell isolated MZP was still developed although the success rate was at times rather low. The number of variables deemed cross-testing to find possible errors in the protocol difficult. It is likely that the low success was due to several factors related to both single-cell isolation and PCR.

Due to the limited temporal occurrence of many MZP species in specific seasons, efforts of obtaining samples of specific species must be focused on bloom periods (Ki, 2004) since the cultivation of MZP taxa has been proven to be a difficult task (Ki, 2004). Furthermore, there are additional difficulties related to the physical isolation of MZP cells. Imagery of cells before isolation was a challenging step, especially with fragile aloricate ciliates and athecate dinoflagellates which were prone to cell lysis during handling. The photography of live specimens is proven to be a useful addition to morphological identification from fixed material, due to many species specific MZP traits being only visible in live or cytologically stained specimens (Agatha, 2011). This is supported by the findings in this project, as photography of specimens isolated proved to be useful for post-hoc identification. Although it is preferable to have a picture identity of all isolated specimens, a protocol where specimens were identified against reference images before isolation proved to be useful in some cases.

Most of the successfully amplified samples were washing using MQ-water. Washing of cells in single-cell isolation is considered as important as external contaminants on MZP cells such as suspended debris among other material can act as inhibitors in DNA amplification reactions (Gao, 2017). Washing solutions such as autoclaved seawater and TE-buffer have been previously used in single-cell isolation protocols (Edwardsen et al. 2003; Ki et al. 2004). It is not certain whether MQ-water is superior or inferior to the other washing solutions tested due to not being cross tested properly with the other steps in the protocol. However, 26.5 percent of the samples were successfully amplified when washed using MQ-water in comparison to the much fewer amplified samples of TE-buffer which proved to not be viable for further use. Evidence of possible contamination from non MZP DNA was observed only in one sequence. It is uncertain whether this could be avoided with a different washing

step. Of all the different iterations of the protocol, the protocol version using PCR master mix as a final cell sample preservative and storing agent was most successful. This method needed the least amount of sample preparation before amplification with only the addition of polymerase and MQ-water. In addition, there was no potential loss of DNA through additional pipetting since PCR reactions were run in the sampling tubes.

In addition to contamination from free DNA and external contaminants, it is also a risk of amplifying DNA from ingested prey organisms (Gao, 2017). In this study, the BLAST results show only one case of evident contamination with the amplification of diatom DNA instead of DNA from the target MZP cell.

Storage of samples in Lugol's iodine solution is a common for MZP. Single-cell isolation was demonstrated to be feasible from Lugol preserved specimens, although single-cell PCR had low success. The sequence retrieved from a Lugol isolate of *L. strobila* was determined as low quality. The single cell isolation technique used a thiosulphate solution to neutralise iodine which is a fixation agent in Lugol's iodine solution. Lugol's iodine solution is known to have an inhibitory effect on PCR reactions as iodine is thought to be embedded in molecular structure of DNA (Auinger et al. 2008). According to Auinger et al. (2008), adding thiosulphate to PCR master mix can help neutralise the inhibiting effects of iodine. The use of thiosulphate in this experiment was as a washing solution which proved to have visual effects. The evident low quality of the sequence obtained with this method may suggest an effect from thiosulphate. although iodine molecules embedded within the DNA structure may not have been sufficiently neutralised, therefore inhibiting amplification.

While successful protocols for single-cell isolation and DNA amplification can be developed, there is still need for improvement on increase the success rate, making the method less cost and labour intensive. The low PCR success in the final protocol could be further improved by optimisation in both the isolation and the amplification itself. While the isolation is adequate for robust organisms such as tintinnids there is a need to modify the protocol to achieve better success with fragile specimens e.g. oligotrich ciliates. Further testing and development of primers could help improving the success rate as for this broad target group. It is likely that some MZP groups require more specific primers although these groups could not be identified in this project. Isolation from Lugol's iodine solution showed promising results in this study and thus, developing a working protocol for this kind of isolation would be a big

breakthrough in terms of effectiveness of single-cell isolation. This would allow to bypass the seasonality aspects in addition to the time constraint of working with live sample material. It is also likely that single-cell isolation from Lugol's iodine solution would improve the ability to successfully isolate DNA from fragile taxa.

## 5. Conclusion and outlook

While successful protocols for single-cell isolation and DNA amplification can be developed, there is still need for improvement on increase the success rate, making the method less cost and labour intensive. The low PCR success in the final protocol could be further improved by optimisation in both the isolation and the amplification itself. While the isolation is adequate for robust organisms such as tintinnids there is a need to modify the protocol to achieve better success with fragile specimens e.g. oligotrich ciliates. Further testing and development of primers could help improving the success rate as for this broad target group. It is likely that some MZP groups require more specific primers although these groups could not be identified in this project. Isolation from Lugol's iodine solution showed promising results in this study and thus, developing a working protocol for this kind of isolation would be a big breakthrough in terms of effectiveness of single-cell isolation. This would allow to bypass the seasonality aspects in addition to the time constraint of working with live sample material. It is also likely that single-cell isolation from Lugol's iodine solution would improve the ability to successfully isolate DNA from fragile taxa.

Ichthyoplankton in the earliest stages have been found to consume armoured MZP (Montagnes et al., 2010). It is arguable whether this is due to prey preferences or due to overrepresentation of more robust organisms in the digestive tracts of fish larvae (Montagnes et al., 2010). Due to the size and digestion rates it is difficult to perform gut content analysis on fish larvae and especially the earlier stages which are thought to be the most dependent on MZP as prey (Montagnes et al., 2010; Bils et al., 2014; Bils et al., 2017). The use of molecular tools for gut content analysis may prove to be an important tool when morphological methods fall short (Roslin & Majaneva, 2016). The trophic link between MZP and ichthyoplankton has been recognised although little is known about the nature of this link. It is argued that application of molecular tools to identify MZP content in the digestive tracts of fish larvae is a possible method to help shedding light on this interaction in the trophic food

web (Montagnes et al., 2010) and the flow of matter and energy from the base of the food web to higher trophic levels (Mitra et al., 2014).

In general comparison to the monitoring series, molecular data shows a big discrepancy in coverage of the total MZP community. It is, however, evident that it was possible to obtain data from arguably some of the key taxa found in the time series. The taxa identified by molecular methods would be significant target taxa in terms of biomonitoring, food web ecology and general studies of the MZP community. Obtaining molecular data from Trondheimsfjorden is an important step towards understanding local and global patterns of MZP communities. Although this group of plankton has been studied extensively with morphological identification methods work still remains towards uncovering many of the aspects of MZP and their role in planktonic communities.

## 6. Literature

Aberle, N., Lengfellner, K., & Sommer, U. (2007). Spring bloom succession, grazing impact and herbivore selectivity of ciliate communities in response to winter warming. *Oecologia*, 150(4), 668-681.

Agatha, S. (2011). Global diversity of aloricate Oligotrichea (Protista, Ciliophora, Spirotricha) in marine and brackish sea water. *PloS one*, 6(8), e22466.

Agatha, S., Strüder-Kypke, M. C., & Beran, A. (2004). Morphologic and genetic variability in the marine planktonic ciliate *Laboea strobila* Lohmann, 1908 (Ciliophora, Oligotrichia), with notes on its ontogenesis. *Journal of Eukaryotic Microbiology*, 51(3), 267-281.

Altschul, S.F., Gish, W., Miller, W., Myers, E.W. & Lipman, D.J. (1990) "Basic local alignment search tool." *Journal of Molecular Biology* 215:403-410.

Auinger, B. M., Pfandl, K., & Boenigk, J. (2008). Improved methodology for identification of protists and microalgae from plankton samples preserved in Lugol's iodine solution: combining microscopic analysis with single-cell PCR. *Applied Environmental Microbiology*, 74(8), 2505-2510.

Azam, F., Fenchel, T., Field, J. G., Gra, J. S., Meyer-Rei, L. A., & Thingstad, F. (1983). The ecological role of water-column microbes in the sea. *Marine Ecology Progress Series*, 10, 257-263.

Bakken, T. 2000. Topografien i Trondheimsfjorden. S. 12-18 i Sakshaug, E og Sneli, J.-A. (red.): *Trondheimsfjorden*. Tapir forlag, Trondheim, pp. 336

Bakken, T. Holthe, T. Sneli, J.-A. (2000). Strøm, vannutveksling og tidevann. p. 42-58 i Sakshaug, E og Sneli, J.-A. (red.): *Trondheimsfjorden*. Tapir forlag, Trondheim, 336 sider.

Bils, F., Moyano, M., Aberle, N., Hufnagl, M., Alvarez-Fernandez, S. & Peck, M. A. (2017). Exploring the microzooplankton-ichthyoplankton link: a combined field and modeling study of Atlantic herring (*Clupea harengus*) in the Irish Sea. *Journal of Plankton Research*, 39, 147-163.

Bils, F., Moyano, M., Aberle, N., Van Damme, C. J. G., Nash, R. D. M., Kloppmann, M., Loots, C. & Peck, M. A. 2019. Broad-scale distribution of the winter protozooplankton community in the North Sea. *Journal of Sea Research*, 144, 112-121.

Calbet, A. (2008). The trophic roles of microzooplankton in marine systems. *ICES Journal of Marine Science*, 65(3), 325-331.

- Calbet, A., & Alcaraz, M. (2009). Microzooplankton, key organisms in the pelagic food web. *Fisheries and Aquaculture*, 5, 227-242.
- Calbet, A., & Landry, M. R. (2004). Phytoplankton growth, microzooplankton grazing, and carbon cycling in marine systems. *Limnology and Oceanography*, 49(1), 51-57.
- Edvardsen, B., Shalchian-Tabrizi, K., Jakobsen, K. S., Medlin, L. K., Dahl, E., Brubak, S., & Paasche, E. (2003). Genetic variability and molecular phylogeny of *Dinophysis* species (dinophyceae) from norwegian waters inferred from single cell analyses of rDNA 1. *Journal of Phycology*, 39(2), 395-408.
- Felsenstein J. (1985). Confidence limits on phylogenies: An approach using the bootstrap. *Evolution* 39:783-791.
- Feng, M., Zhang, W., Wang, W., Zhang, G., Xiao, T., & Xu, H. (2015). Can tintinnids be used for discriminating water quality status in marine ecosystems?. *Marine Pollution Bulletin*, 101(2), 549-555.
- Gribble, K. E., & Anderson, D. M. (2007). High intraindividual, intraspecific, and interspecific variability in large-subunit ribosomal DNA in the heterotrophic dinoflagellates *Protoperidinium*, *Diplopsalis*, and *Preperidinium* (Dinophyceae). *Phycologia*, 46(3), 315-324.
- Hall, T.A. 1999. BioEdit: a user-friendly biological sequence alignment editor and analysis program for Windows 95/98/NT. *Nucleic Acids Symposium*. Ser. 41:95-98.
- Hebert, P. D., Cywinska, A., Ball, S. L., & Dewaard, J. R. (2003). Biological identifications through DNA barcodes. *Proceedings of the Royal Society of London. Series B: Biological Sciences*, 270(1512), 313-321.
- Hillebrandt, H., Dürselen, C. D., Kirschtel, D., Pollinger, U., & Zohary, T. (1999). Biovolume calculation for pelagic and benthic microalgae. *Journal of Phycology*, 35(2), 403-424.
- Jeong, H. J., Du Yoo, Y., Kim, S. T., & Kang, N. S. (2004). Feeding by the heterotrophic dinoflagellate *Protoperidinium bipes* on the diatom *Skeletonema costatum*. *Aquatic Microbial Ecology*, 36(2), 171-179.
- Jeong, H. J., & Latz, M. I. (1994). Growth and grazing rates of the heterotrophic dinoflagellates *Protoperidinium* spp. on red tide dinoflagellates. *Marine Ecology-Progress Series*, 106, 173-173.
- Johnson, M. D., & Stoecker, D. K. (2005). Role of feeding in growth and photophysiology of *Myrionecta rubra*. *Aquatic Microbial Ecology*, 39(3), 303-312.
- Karlson, B., Cusack, C., & Bresnan, E. (2010). Microscopic and molecular methods for quantitative phytoplankton analysis. Paris: UNESCO. pp 13–20.

- Katoh, K., Rozewicki, J., & Yamada, K. D. (2017). MAFFT online service: multiple sequence alignment, interactive sequence choice and visualization. *Briefings in bioinformatics*, 30, 3059
- Ki, J. S., Jang, G. Y., & Han, M. S. (2004). Integrated method for single-cell DNA extraction, PCR amplification, and sequencing of ribosomal DNA from harmful dinoflagellates *Cochlodinium polykrikoides* and *Alexandrium catenella*. *Marine Biotechnology*, 6(6), 587-593.
- Kraberg, A., Baumann, M., & Dürselen, C. D. (2010). Coastal phytoplankton: photo guide for Northern European seas. Pfeil Verlag. Munchen, pp. 204.
- Kumar S., Stecher G., Li M., Knyaz C., and Tamura K. (2018). MEGA X: Molecular Evolutionary Genetics Analysis across computing platforms. *Molecular Biology and Evolution* 35:1547-1549.
- Larinck, O. & Westheide, W. (2006): Coastal Plankton – Photo guide for European seas. Pfeil, Verlag, München, 204 pp.
- Lin, S., Zhang, H., Hou, Y., Miranda, L., & Bhattacharya, D. (2006). Development of a dinoflagellate-oriented PCR primer set leads to detection of picoplanktonic dinoflagellates from Long Island Sound. *Applied. Environmental. Microbiology*, 72(8), 5626-5630.
- Löder, M. G. J., & Haunost, M., (2009). Marine microzooplankton of the North Sea. Alfred-Wegener-Institut: Helmholtz-Zentrum für Polar-und Meeresforschung.
- Löder, M. G. J., Kraberg, A. C., Aberle, N., Peters, S., & Wiltshire, K. H. (2012). Dinoflagellates and ciliates at Helgoland roads, North Sea. *Helgoland Marine Research*, 66(1), 11.
- Marín, I., Aguilera, A., Reguera, B., & Abad, J. P. (2001). Preparation of DNA suitable for PCR amplification from fresh or fixed single dinoflagellate cells. *BioTechniques*, 30(1), 88-93.
- Montagnes, D. J. (1996). Growth responses of planktonic ciliates in the genera *Strobilidium* and *Strombidium*. *Marine Ecology Progress Series*, 130, 241-254.
- Montagnes, D. J., Allen, J., Brown, L., Bulit, C., Davidson, R., Díaz-Ávalos, C., ... & Sanders, R. (2008). Factors controlling the abundance and size distribution of the phototrophic ciliate *Myrionecta rubra* in open waters of the North Atlantic. *Journal of Eukaryotic Microbiology*, 55(5), 457-465.
- Montagnes, D. J., Dower, J. F., & Figueiredo, G. M. (2010). The Protozooplankton–Ichthyoplankton Trophic Link: An Overlooked Aspect of Aquatic Food Webs 1. *Journal of Eukaryotic Microbiology*, 57(3), 223-228.

- Nei M. & Kumar S. (2000). *Molecular Evolution and Phylogenetics*. Oxford University Press, New York.
- Pawlowski, J., Audic, S., Adl, S., Bass, D., Belbahri, L., Berney, C., ... & Fiore-Donno, A. M. (2012). CBOL protist working group: barcoding eukaryotic richness beyond the animal, plant, and fungal kingdoms. *PLoS biology*, *10*(11), e1001419.
- Pomeroy, L. R., Williams, P. J., Azam, F., & Hobbie, J. E. (2007). The microbial loop. *Oceanography*, *20*(2), 28-33.
- Roslin, T., & Majaneva, S. (2016). The use of DNA barcodes in food web construction—terrestrial and aquatic ecologists unite! *Genome*, *59*(9), 603-628.
- Rueden, C. T, Schindelin, J. & Hiner, M. C. et al. (2017), “ImageJ2: ImageJ for the next generation of scientific image data”, *BMC Bioinformatics* 18:529, PMID 29187165, doi:10.1186/s12859-017-1934-z
- Sieburth, J. M., Smetacek, V., & Lenz, J. (1978). Pelagic ecosystem structure: Heterotrophic compartments of the plankton and their relationship to plankton size fractions 1. *Limnology and oceanography*, *23*(6), 1256-1263.
- Kasai, F. (2012). Evaluating the ribosomal internal transcribed spacer (ITS) as a candidate dinoflagellate barcode marker. *PLoS One*, *7*(8), e42780.
- Smetacek, V. (1981). The annual cycle of protozooplankton in the Kiel Bight. *Marine Biology*, *63*(1), 1-11.
- Stoecker, D. K., Michaels, A. E., & Davis, L. H. (1987). Large proportion of marine planktonic ciliates found to contain functional chloroplasts. *Nature*, *326*(6115), 790.
- Sun, J., & Liu, D. (2003). Geometric models for calculating cell biovolume and surface area for phytoplankton. *Journal of Plankton Research*, *25*(11), 1331-1346.
- Tokle, E. (1999). Forekomst av dyreplankton i Trondheimsfjorden med fokus på stoffomsetningen. Norwegian University of Science and Technology. MSc thesis, pp. 168
- Töbe, K., Meyer, B., & Fuentes, V. (2010). Detection of zooplankton items in the stomach and gut content of larval krill, *Euphausia superba*, using a molecular approach. *Polar Biology*, *33*(3), 407-414.
- Widdicombe, C. E., Archer, S. D., Burkill, P. H., & Widdicombe, S. (2002). Diversity and structure of the microplankton community during a coccolithophore bloom in the stratified northern North Sea. *Deep Sea Research Part II: Topical Studies in Oceanography*, *49*(15), 2887-2903.

Yang, J., Löder, M. G. J., & Wiltshire, K. H. (2014). A survey of ciliates at the long-term sampling station “Helgoland Roads”, North Sea. *Helgoland Marine Research*, 68(2), 313

## Appendix A

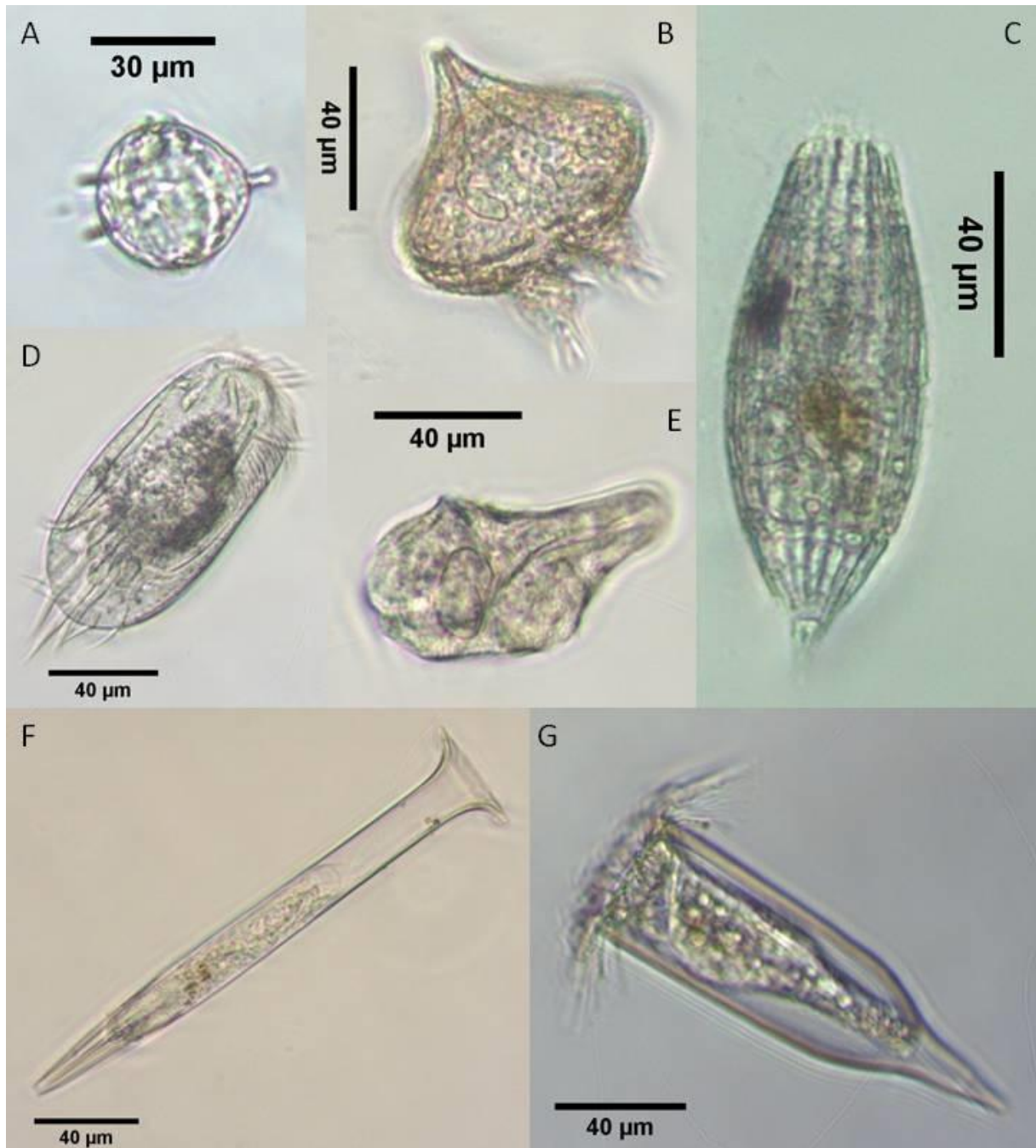


Figure 12: Live specimens of dominant species from the autumn 2018 season. Specimens were isolated with single-cell isolation. *Protoperidinium* sp. (A), *Protoperidinium* sp. (B), *Tiarina* cf. *fuscus* (C), *Euplotes* sp. (D), *Gyrodinium* cf. *spirale* (E), *Salpingella* sp. (F) and undetermined tintinnid ciliate (G). Photos taken with Leica DM IRB inverted microscope (20x objective).

